



Natural Resources
Canada

Ressources naturelles
Canada

**GEOLOGICAL SURVEY OF CANADA
OPEN FILE 8496**

**U-Pb geochronology, geochemistry, and geological setting
of Devonian and Eocene granitic intrusions of northern
Yukon and adjacent Alaska: site and sample descriptions,
data tables, and imagery**

**L.S. Lane, J.K. Mortensen, J.H. Dover, R.J. Thériault, K. Bell,
and J. Blenkinsop**

2018

Canada



GEOLOGICAL SURVEY OF CANADA OPEN FILE 8496

U-Pb geochronology, geochemistry, and geological setting of Devonian and Eocene granitic intrusions of northern Yukon and adjacent Alaska: site and sample descriptions, data tables, and imagery

**L.S. Lane, J.K. Mortensen, J.H. Dover, R.J. Thériault, K. Bell,
and J. Blenkinsop**

2018

© Her Majesty the Queen in Right of Canada, as represented by the Minister of Natural Resources, 2018

Information contained in this publication or product may be reproduced, in part or in whole, and by any means, for personal or public non-commercial purposes, without charge or further permission, unless otherwise specified.

You are asked to:

- exercise due diligence in ensuring the accuracy of the materials reproduced;
- indicate the complete title of the materials reproduced, and the name of the author organization; and
- indicate that the reproduction is a copy of an official work that is published by Natural Resources Canada (NRCan) and that the reproduction has not been produced in affiliation with, or with the endorsement of, NRCan.

Commercial reproduction and distribution is prohibited except with written permission from NRCan. For more information, contact NRCan at nrcan.copyrightdroitdauteur.rncan@canada.ca.

Permanent Link: <https://doi.org/10.4095/313230>

This publication is available for free download through GEOSCAN (<http://geoscan.nrcan.gc.ca/>).

Recommended citation

Lane, L.S., Mortensen, J.K., Dover, J., Thériault R.J., Bell, K., and Blenkinsop, J., 2018. U-Pb geochronology, geochemistry, and geological setting of Devonian and Eocene granitic intrusions of northern Yukon and adjacent Alaska: site and sample descriptions, data tables, and imagery; Geological Survey of Canada, Open File 8496, 1 .zip file. <https://doi.org/10.4095/313230>

Publications in this series have not been edited; they are released as submitted by the author.

ABSTRACT

New data tables, figures and imagery from northern Yukon and adjacent Arctic Alaska document the field relationships, lithologies, petrography, geochronology and geochemistry of a suite of Late Devonian granites and syenite, as well as an Eocene syenite. These data sets support an interpretation and synthesis of the tectonic implications of these magmatic episodes that will be published in a peer-reviewed journal. Included as Appendix A, is a summary of archival Rb-Sr geochronological datasets that have not been published previously.

Appendix B contains five data tables that provide complete documentation supporting the results of the current study, together with a substantial amount of previously unpublished geochronology and geochemistry data.

INTRODUCTION

This Open File contains geochronology and geochemistry data in Appendices A and B, together with contextual information for a suite of Devonian and Eocene felsic intrusions located in northernmost Yukon and adjacent Alaska (Fig. 1). The contextual data include site and sample descriptions, sample and field photographs, micrographs, figures, locality information and maps.

The tables and descriptive figures provide supplementary data in support of the interpretations, discussions and syntheses presented in a journal publication (Lane and Mortensen, 2019).

The ages, geochemistry and tectonic implications of these intrusive bodies provide important new information that constrains syntheses of the Devonian, in particular, and also the Paleogene structural evolution in northwestern Canada and adjacent Arctic Alaska.

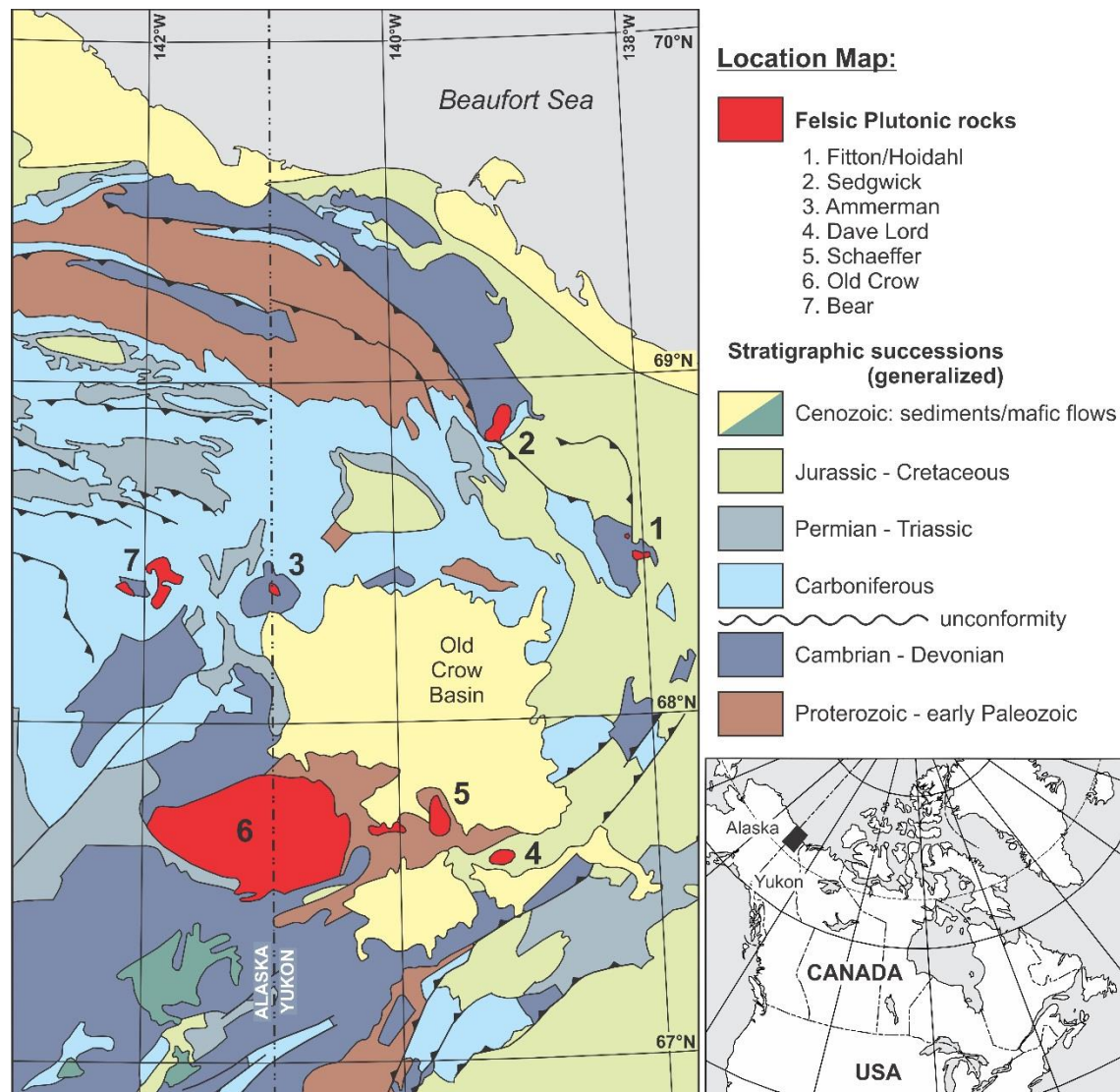


Figure 1. Generalized location map showing the felsic intrusions described herein and reported on by Lane and Mortensen (2019).

SITE AND SAMPLE DESCRIPTIONS

Specific localities of all geochemistry and geochronology samples in this study are tabulated in Appendix Table B1. Figures and Captions are in-line with the text, whereas large-format geochemistry and geochronology data tables are in Appendix B.

Mount Fitton Granite

The Mount Fitton granite (Fig. 1) intrudes Paleozoic strata and is unconformably overlain by Cretaceous rocks (Figs. 2 and 3). However, its base is a low angle thrust fault (Figs. 2 and 4).

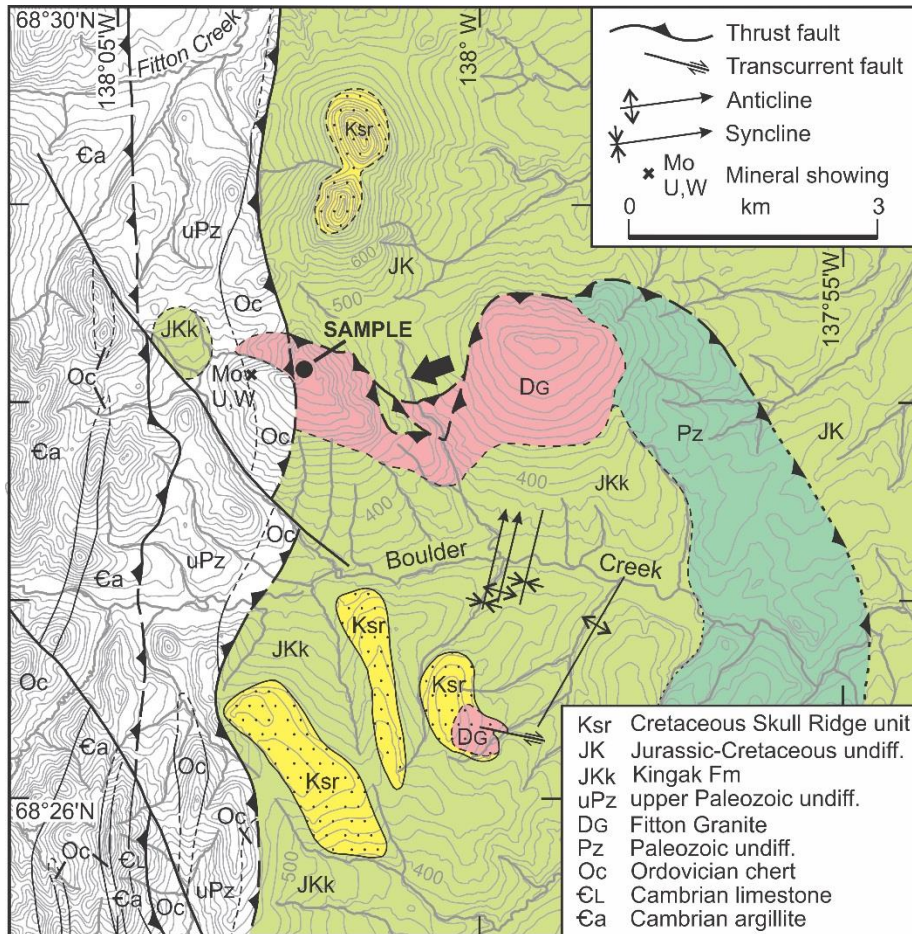


Figure 2. Geological setting of the Mount Fitton granite. The geology is modified from Cecile and Lane (1991) and unpublished data. Arrow shows the approximate view displayed in Figure 4 (below).

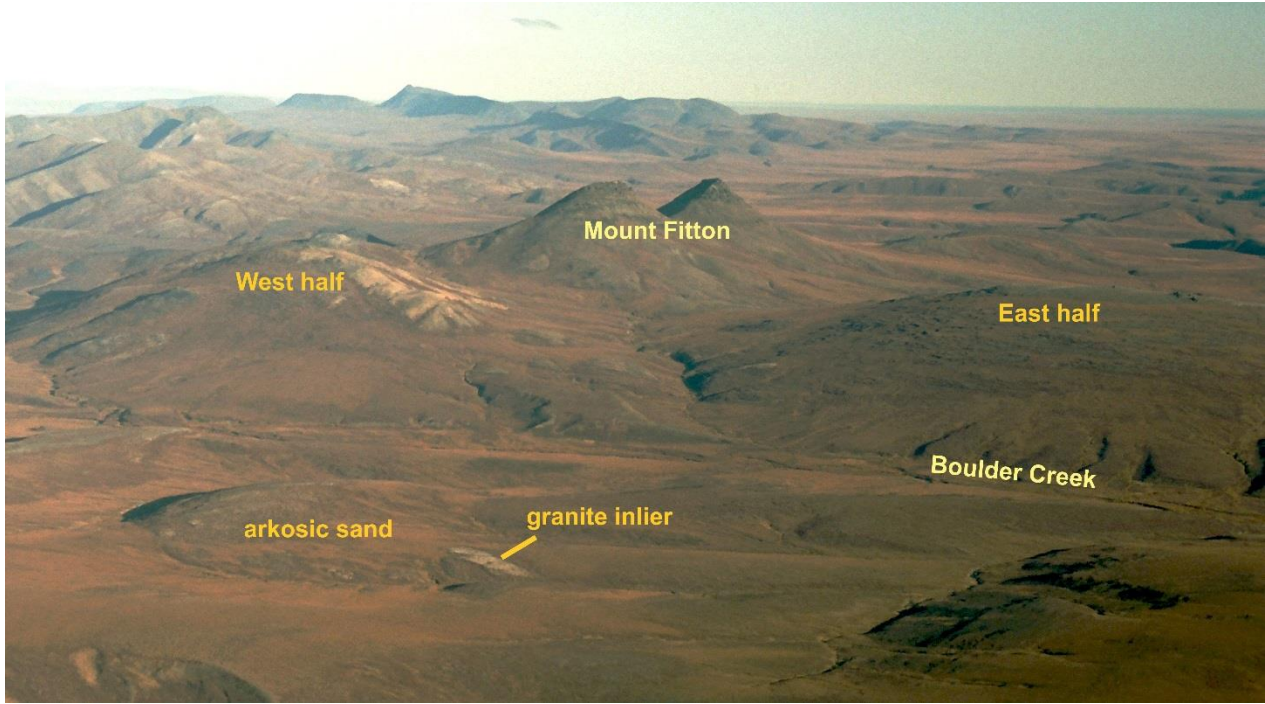


Figure 3. Aerial view looking northward at Mount Fitton granite, with west and east granite exposures and the granite inlier south of Boulder Creek (photo 2003-P2-21). The adjacent arkosic sand is a granite wash exposure, mapped as Cretaceous (Albian) in age (Unit Ksr, Norris, 1981a). In the background, behind the “west half” of the Fitton granite are imbricated ridges of Cambrian to Devonian clastic and carbonate rocks of the Barn Mountains (Cecile and Lane, 1991). The twin peaks of Mount Fitton are composed of coarse clastic strata of an Albian flysch unit against which the Devonian granites, together with their enclosing early Paleozoic strata, were faulted during latest Cretaceous and Paleogene tectonism (Lane, 1998).

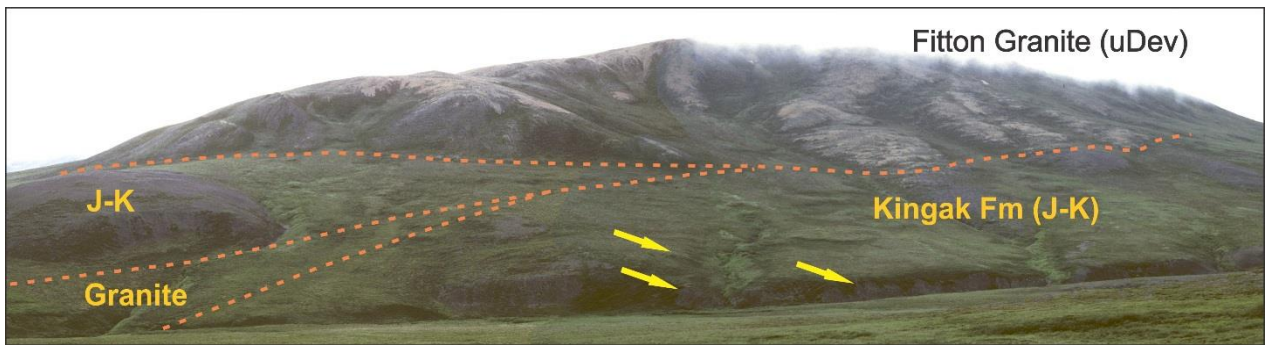


Figure 4. Photomosaic view westward at basal thrust-faulted contact of the Fitton Granite (uDev) lying on northwest-dipping shale and siltstone ascribed to the Kingak Formation (Jurassic - Early Cretaceous). Yellow arrows indicate visible bedding with apparent dips $\sim 20^\circ$ to the north. Field of view is ~ 1200 m.

Hoidahl Cupola

Hoidahl Cupola intrudes the northeastern part of Barn Uplift (Fig. 1). The uplift is underlain by a significant basal thrust fault (Fig. 5). Also, two areas with common granitic dyke occurrences 3 km to the south were mapped by Cecile and Lane (1991). These dyke occurrences would be consistent with the interpretation that Hoidahl Cupola represents the upper part of an epizonal pluton as suggested by Burwash (1997), and implies a wider subsurface extent to the local magmatism. This pluton is associated with gossan alteration zones (Figs. 6 and 7) which contain molybdenum and tungsten mineralization (Findlay and Caine, 1981).

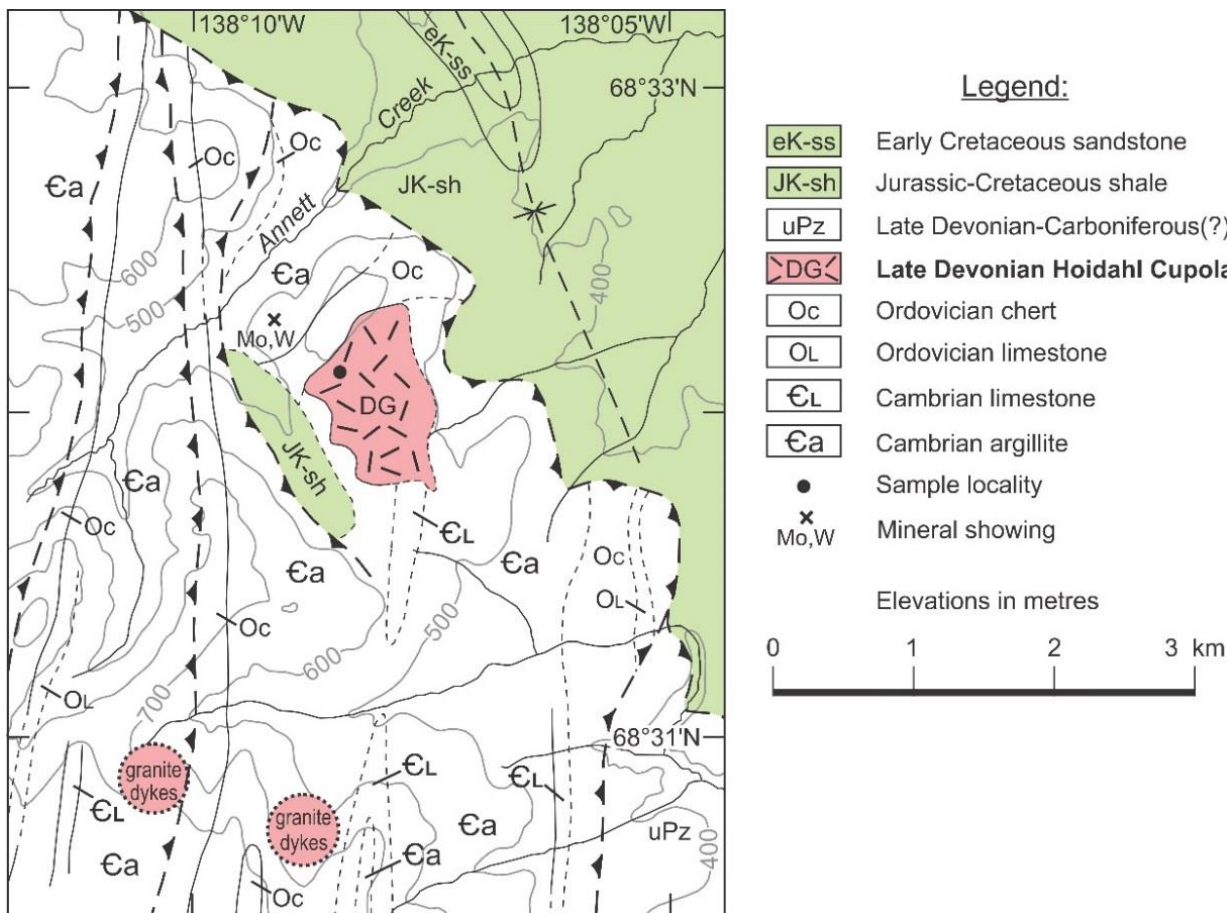


Figure 5. Hoidahl Cupola showing the two areas with common granitic dyke occurrences 3 km to the south (modified from Cecile and Lane, 1991).



Figure 6. Aerial view toward the east at a prominent orange gossan on the north margin of Hoidahl Cupola (photo 2018-DSC_10046). The adjacent dominantly light grey low-elevation exposure is granite, whereas the dominant peak is mapped as Ordovician chert.



Figure 7. Hoidahl cupola forms much of the horseshoe-shaped hill (~2 km across) in the foreground, with early Paleozoic strata dominated by Cambrian argillite with light-weathering limestone, and dark Ordovician chert in north-trending ridges behind (see Cecile and Lane, 1991). Orange gossans are visible at the lower left corner. Aerial view looking westward (1988-02-06).

Sedgwick Granite

Sedgwick granite is located at the eastern limit of Paleozoic and Proterozoic exposures of the British mountains (Fig. 1). It intrudes a carbonate-clastic succession on its western flank and chert-argillite successions on the eastern flank (Fig. 8). The intruded rocks were deformed into tight folds prior to intrusion. The chert-argillite succession strikes directly into the pluton, and has steep dips. It may correlate with Road River basinal facies mapped farther northwest along strike in the British Mountains (Lane, 1991; Lane et al., 1995), and to the southeast in the Barn Mountains (Cecile and Lane, 1991). The carbonate-clastic succession underlies the latest Proterozoic to Cambrian Neruokpuk Formation, a turbiditic sandstone-siltstone succession equivalent to the lower part of the Hyland Group of the Selwyn Basin, and approximately equivalent to the Windermere Grits of the northern Canadian Cordillera (Lane, 1991; 2007; Lane et al., 2016). As is the case for Mt. Fitton, Sedgwick granite shows no indication of a ductile fabric correlative with those early structures. In at least two locations, large garnet-epidote skarn inclusions within the granite indicate partial digestion of carbonate wall rocks (Fig. 9).

Sedgwick granite is locally affected by Cretaceous-Paleogene faulting on its north and west sides. At least two east-dipping faults offset the west margin with reverse dip-separation on the order of a few metres (Fig. 8). A moderately northeast-dipping shear zone is exposed in the granite at its north contact and presumably offsets it in an area covered by tundra. Abundant undulatory extinction and deformation lamellae, and a lack of recovery textures, in quartz, combined with highly sericitized and fractured feldspars indicate low temperature and/or high strain-rate deformation. This local shear zone also affects the adjacent Carboniferous succession and is interpreted here as a south-directed thrust fault formed during Late Cretaceous-Paleogene regional deformation (Fig. 8).

Unconformably overlying both the pre-Carboniferous metasedimentary wallrocks and the granite are coarse to fine clastic rocks of the Lower Carboniferous Endicott Group, and limestone of the overlying Lisburne Group (Fig. 8, see Lane and Mortensen, 2019). The limestone appears to lie directly on the granite locally in the southeast. If Endicott Group clastic strata occur below the limestone, they are obscured by the extensive talus developed by the limestone. Note that we also map a minor bedding-parallel fault within the Endicott strata along part of this contact.

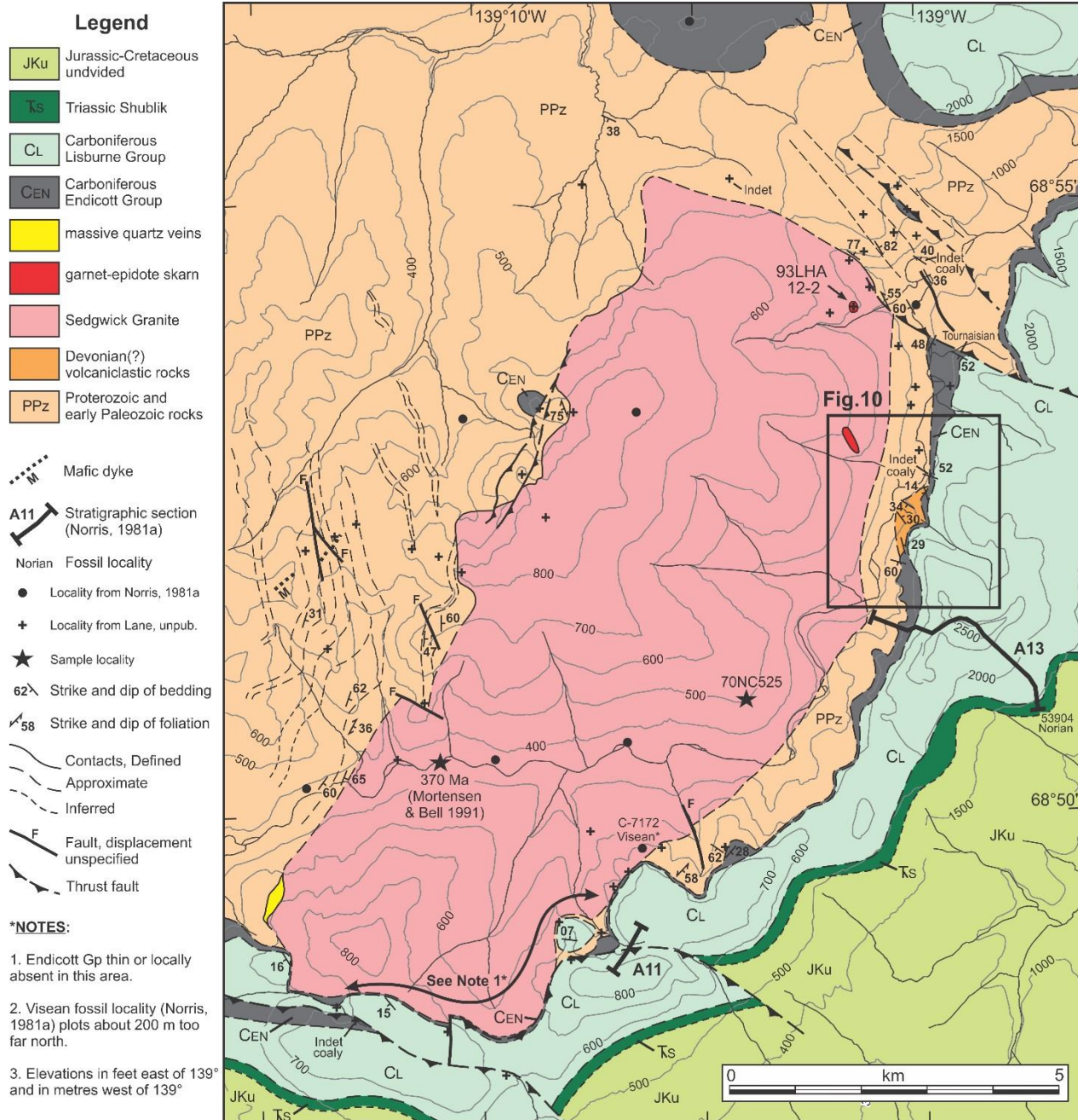


Figure 8. Local geological setting of Sedgwick granite. Compiled from Norris (1981a) and unpublished 1:50,000 scale field maps (by L.S. Lane).



Figure 9. Block of altered carbonate host rock incorporated into the granite. Skarn mineralization includes epidote and garnet. Locality 93LHA12-2 (see Fig. 8), near the northern margin of the pluton. (field photo 93-04-21 scanned from 35 mm slide).

A previously unmapped sedimentary unit that includes volcaniclastic beds is locally preserved in the hinge of an open southeast-plunging syncline that is truncated beneath the overlying Carboniferous succession east of the pluton (Figs. 8, 10, 11). These beds consist of poorly sorted, coarse-grained lithologies rich in angular to sub-rounded rock fragments up to ~3 cm long, and common wispy, highly angular fragments up to ~1 cm long, interpreted to be collapsed pumice fragments (Figs. 12, 13). They are undated; however, their bedding orientations are more similar to that of the overlying Carboniferous succession than to the pre-Carboniferous strata extensively exposed elsewhere (Figs. 8, 10). Also, a nearby aphanitic, nearly black unit approximately 30-50 cm thick that contains mm-scale clear quartz grains and near-euhedral zircon grains, is interpreted as a rhyolitic sill (Figs. 14 to 17). The volcaniclastic beds may represent the remnant of a volcanic edifice related to an earlier phase of magmatism that ultimately produced Sedgwick granite (see Lane and Mortensen, 2019).

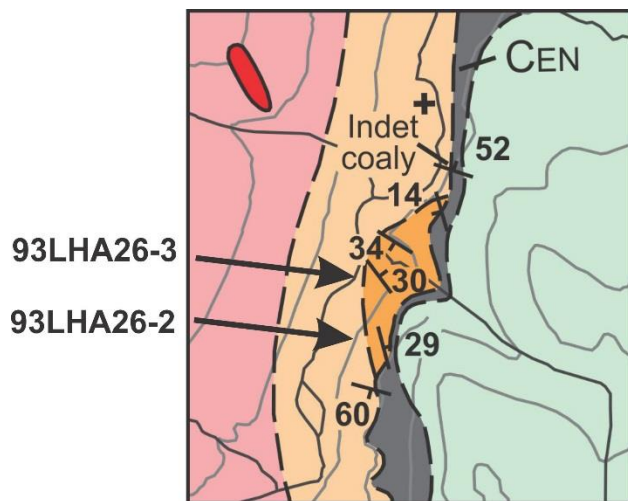


Figure 10. Detail from Sedgwick area map (Fig. 8) showing the locations of stations illustrated in the following field photos and micrographs. Width of view is 2.7 km.

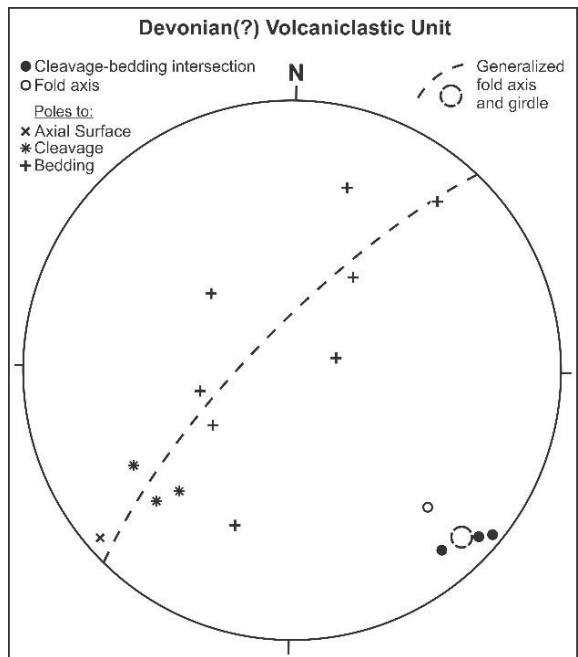


Figure 11. Structural orientations from the volcaniclastic-bearing unit (Fig. 10), unconformably beneath the Carboniferous succession, east of Sedgwick pluton.



Figure 12. Field photo 93-10-20, locality 93LHA26-2 (Fig. 10), scanned from 35mm slide. Clast sizes to ~ 3 cm are visible, light rounded quartz grains and equant to elongate dark grains are common, wispy fiamme are abundant. Image has been digitally sharpened to improve the visibility of fine detail.

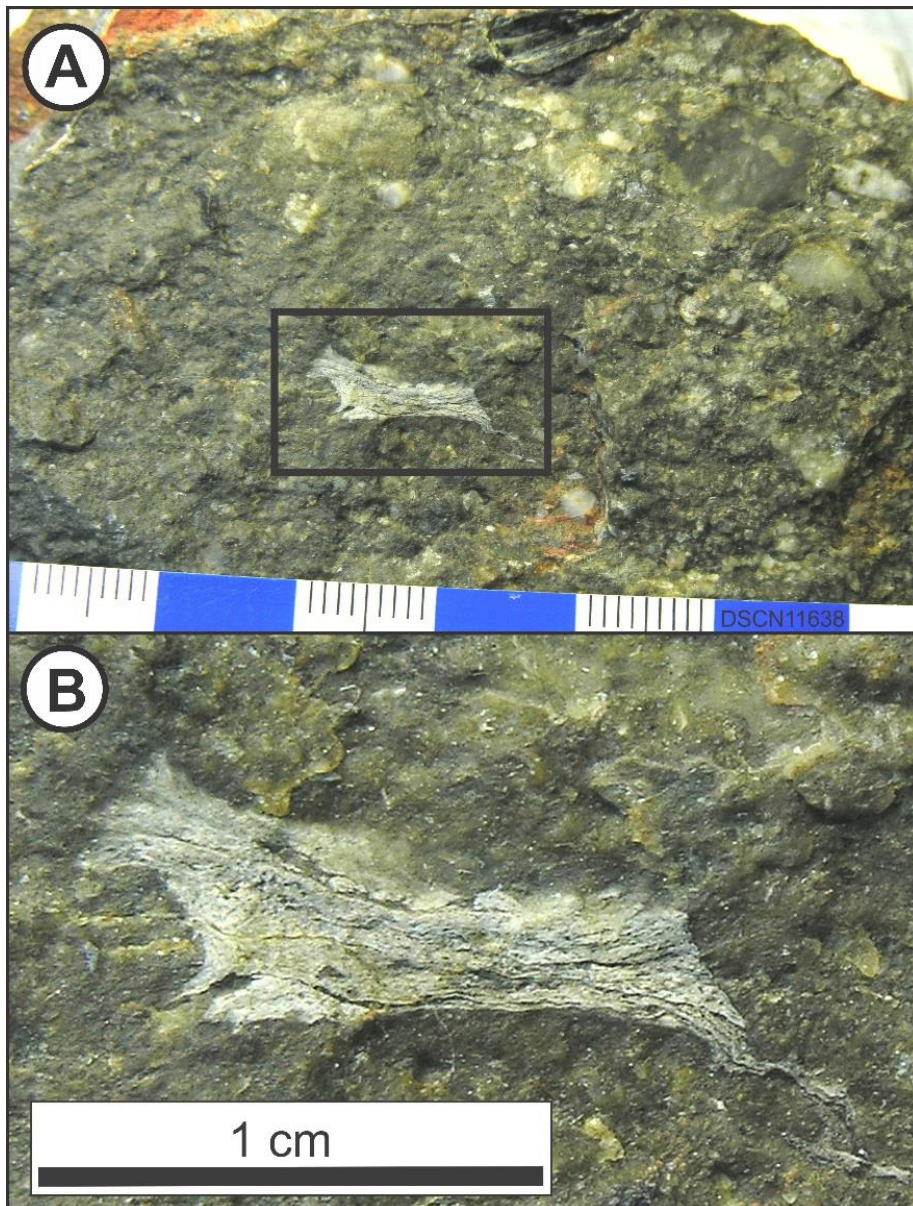


Figure 13. Photograph of hand specimen 93LHA26-2B. (A.) Poorly sorted clastic unit containing a large pumice (?) fragment (outlined); abundant grey to white, sub-angular to well rounded quartz grains; and common dark grey to black finer grains. A large, rounded, dark-grey siltstone clast is visible at the top of the photo. Scale at bottom of photo is in mm and cm. (B) Enlargement of the pumice clast in (A), showing finely laminated structure, highly angular shape and wispy terminations. Image has been digitally sharpened to improve the visibility of fine detail.



Figure 14. Outcrop of a rusty-weathering Devonian(?) sill at station 93LHA26-3 (Fig. 10). In plan view it has a hummocky surface. Several sills are interlayered with cleaved siltstone and slate. Thin section images are shown in Figures 16 and 17. Field photo 93-10-22, scanned from 35 mm slide.



Figure 15. Field photograph 93-10-21, scanned from 35mm slide. Cross-section of sills (dark) exposed in outcrop of cleaved argillite and siltstone. The hummocky surface texture resembles boudinage in cross-section. Along-trend thickening and thinning are also visible. Rock hammer is 34 cm long.



Figure 16. Sampled rhyolitic sill, 93LHA26-3, in thin section. Subhedral to euhedral zircon grains in thin section are ~27 μm long (at left; crossed nicols), ~57 μm long (below; plane light).

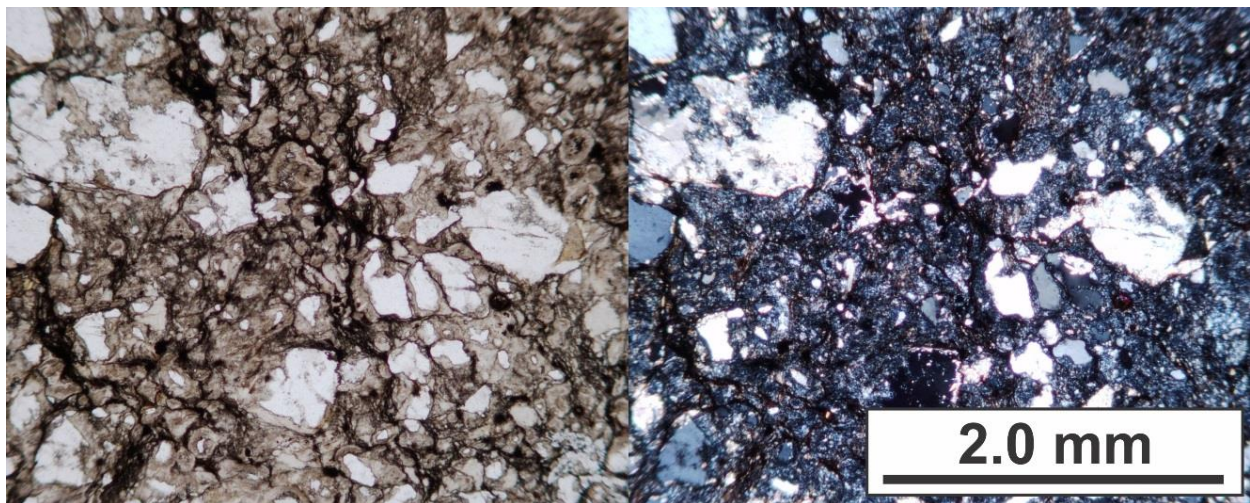
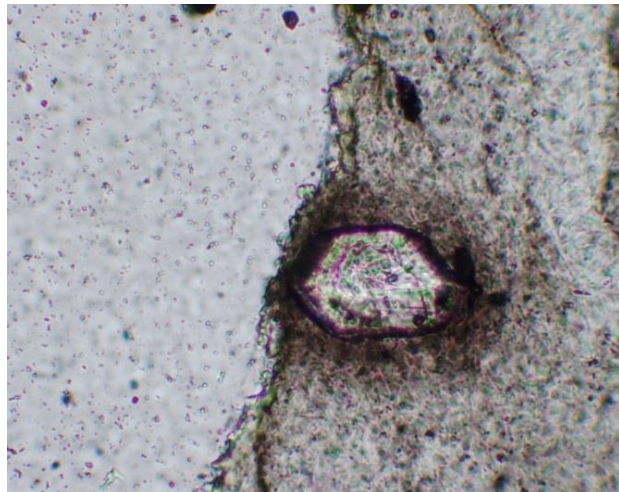


Figure 17. Sample of rhyolitic sill, 93LHA26-3, in thin section: plane polarized light on the left; crossed nicols on the right. Larger grains are quartz, embedded in a grey, microcrystalline groundmass. The quartz is commonly angular to sub-rounded; mono-crystalline to multi-crystalline, some show undulose extinction, or contain elongate subgrains. Grain margins are commonly embayed. A few grains appear to have been broken.

Ammerman Pluton

Ammerman pluton (Figs. 1, 18) is associated with leucocratic quartz porphyry sills(?) although their contacts, and specific relationships to the granite body typically are not exposed.

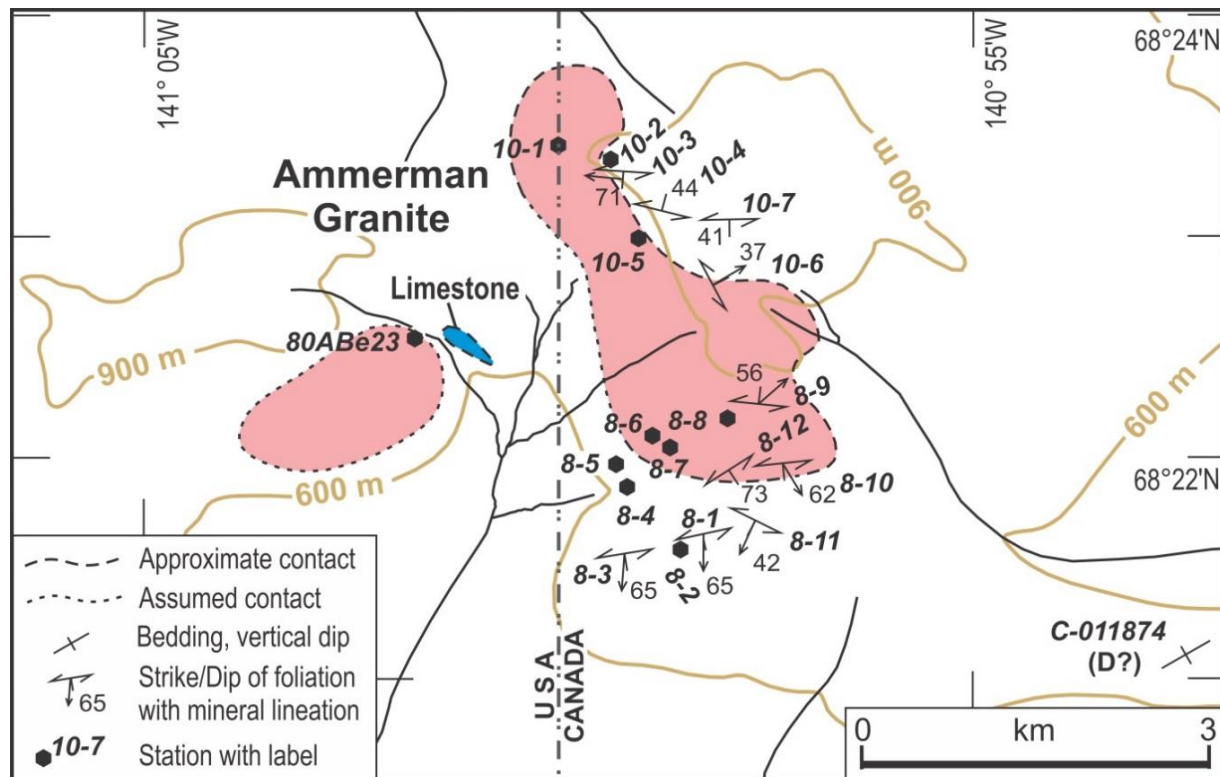


Figure 18. Ammerman Granite, station location map.

Along its northeastern margin, the granite is juxtaposed against a local outlier (or outliers) of dark grey quartzite and conglomerate with minor interbedded shale, resembling Carboniferous Kekiktuk Formation (localities 10-2 and 10-7, Fig. 18). In contrast to the granite and the adjacent (underlying) metasediments (Figs. 19 to 24), the conglomerate shows no evidence of significant bulk strain (Figs. 24, 25). The juxtaposition may represent the sub-Carboniferous unconformity, which must occur in the vicinity because Carboniferous limestones are widely exposed a few (~5 km) distant, to the north, east and south (Norris 1981b). However, a small-displacement, unexposed younger fault also may be responsible for juxtaposing these Carboniferous(?) clastic strata in this poorly exposed area (Fig. 25).

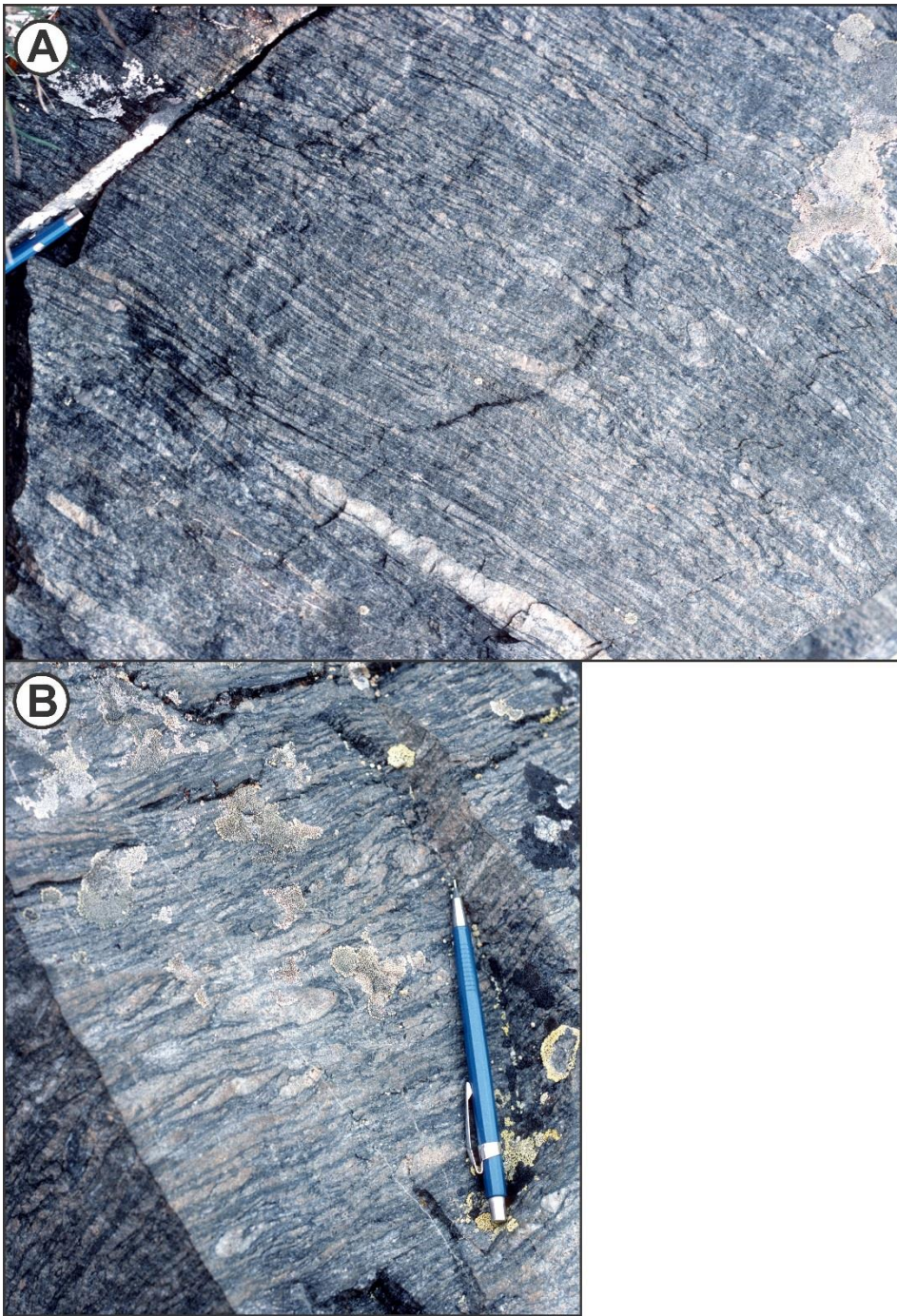


Figure 19. Large frost-heaved block from gneissic zone of Ammerman granite, locality 93LHA8-9, near its east margin. (A), View of joint surface sub-parallel to the plane containing the maximum and minimum strain axes (X-Z). Quartz-feldspar rich boudins are highly elongate, several isoclinal rootless hinges are visible. (B), View of adjacent surface (same block), approximately normal the the maximum strain axis (Y-Z plane). See map for foliation and lineation orientations. Field photos 93-03-12 and -11 (scanned from 35mm slides).



Figure 20. Locality 93LHA8-10, near the southeast margin, a well-developed ductile fabric in the granite is refolded by asymmetric decimetre-scale folds showing a semi-brittle style. In this displaced block, multiple isoclinal, rootless, ductile hinges are well displayed, particularly in the lower part of the block. The two sets of structures developed under distinctly different temperature/strain rate conditions. Field photo 93-03-14 (scanned from 35mm slide).

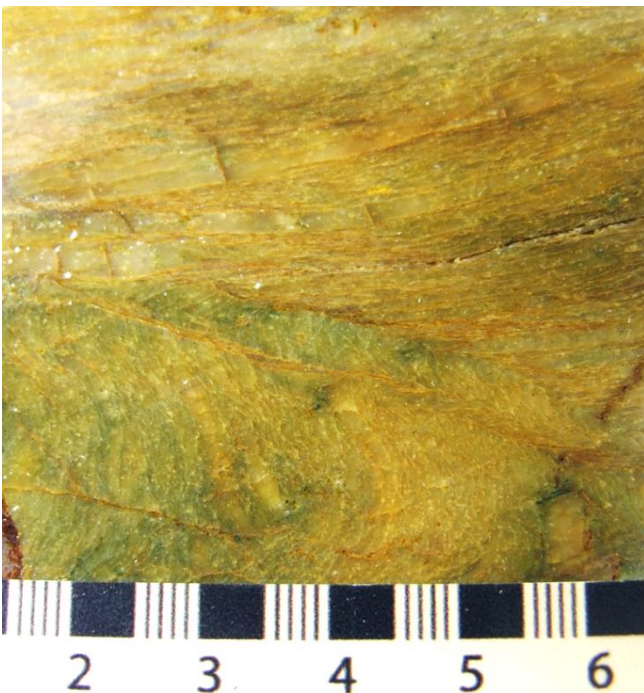


Figure 21. Cut surface of quartzite country rock adjacent to Ammerman pluton. Part of a decimetre-scale minor fold is shown (locality 93LHA10-2). Scale is in centimetres.



Figure 22. Leucocratic quartz porphyry phase (sample 93LHA10-5, collected from talus, downslope from exposed granite) fresh, broken surface. Clear quartz phenocrysts are euhedral to angular. Groundmass is white feldspar and milky quartz. Scale graduations are 1 mm and 5 mm. Field of view is ~5 cm across.

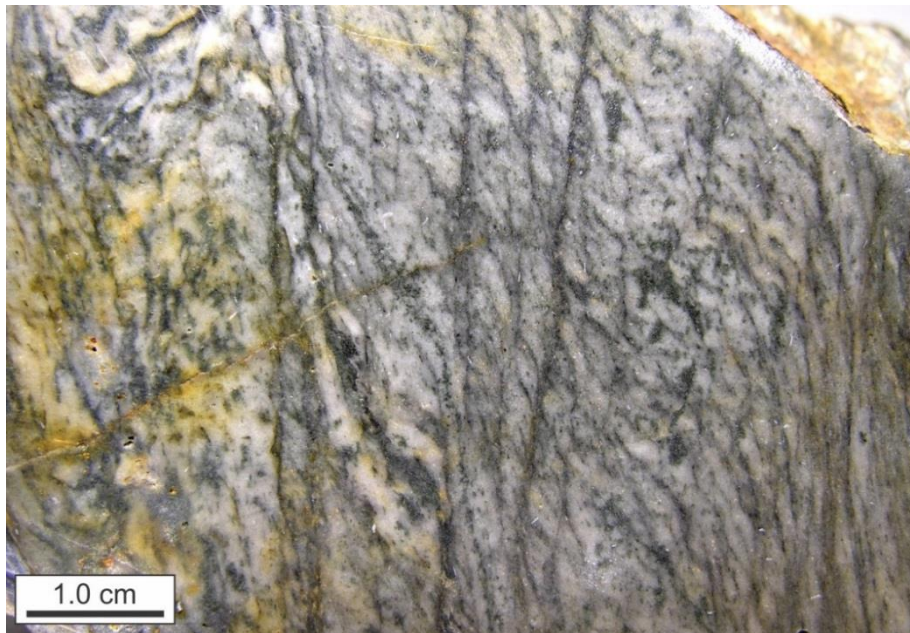


Figure 23. Locality 93LHA10-6. Strained granite sample, with locally developed C-S fabric. Together with the strain gradient at the right edge of the image, they indicate a right-side down shear sense corresponding to a top-to-the SW asymmetry in the outcrop. Whether this cm-scale asymmetry scales up to outcrop or regional significance is uncertain.



Figure 24. Locality 93LHA10-7: Location of unconformity between north-dipping, non-foliated shale, quartzite and conglomerate above; and intensely foliated and crenulated, south-dipping strata below (approximated by dashed line). Yellow circle marks location of shale, sampled for thermal maturity

(sample 10-7A: Ro [equivalent from pyrobitumen] = 3.98%, implying a maximum temperature near $\sim 240^{\circ}\text{C}$); orange circle marks location of conglomerate sample (10-7B, see Fig. 25).



Figure 25. Conglomerate sample (93LHA10-7b, see Fig. 24) fresh, broken surface. Visible are angular to sub-rounded clasts of quartzite, siltstone and dark grey to black argillite. Dominant clast sizes are 0.5 cm to >1 cm length. Although adjacent to the pluton, this unit lacks the intense penetrative strain that is characteristic of the intruded sedimentary rocks elsewhere adjacent to the pluton. Also, the lithology and angular texture are typical of the Kekiktuk Formation (Carboniferous) elsewhere in the area. Although poorly exposed, the distribution of this unit and its juxtaposition adjacent to the metasedimentary succession suggests an unconformable base. Although, a local-scale fault cannot be ruled out in relation to its proximity to the pluton, the strain difference with adjacent metasediments nonetheless suggests an unconformity. Scale bar is in centimetres.

Old Crow Batholith

Old Crow batholith (Fig. 26) lies at the western margin of Old Crow Basin where outcrop exposures are uncommon. The intruded metasedimentary rocks are mapped as Proterozoic in Yukon (Norris, 1981b) and Paleozoic in Alaska (Brosgé and Reiser, 1969). They include quartzites, siltstones, argillaceous rocks and minor carbonates. Primary sedimentary textures are commonly preserved, although localized high strain zones are exposed.

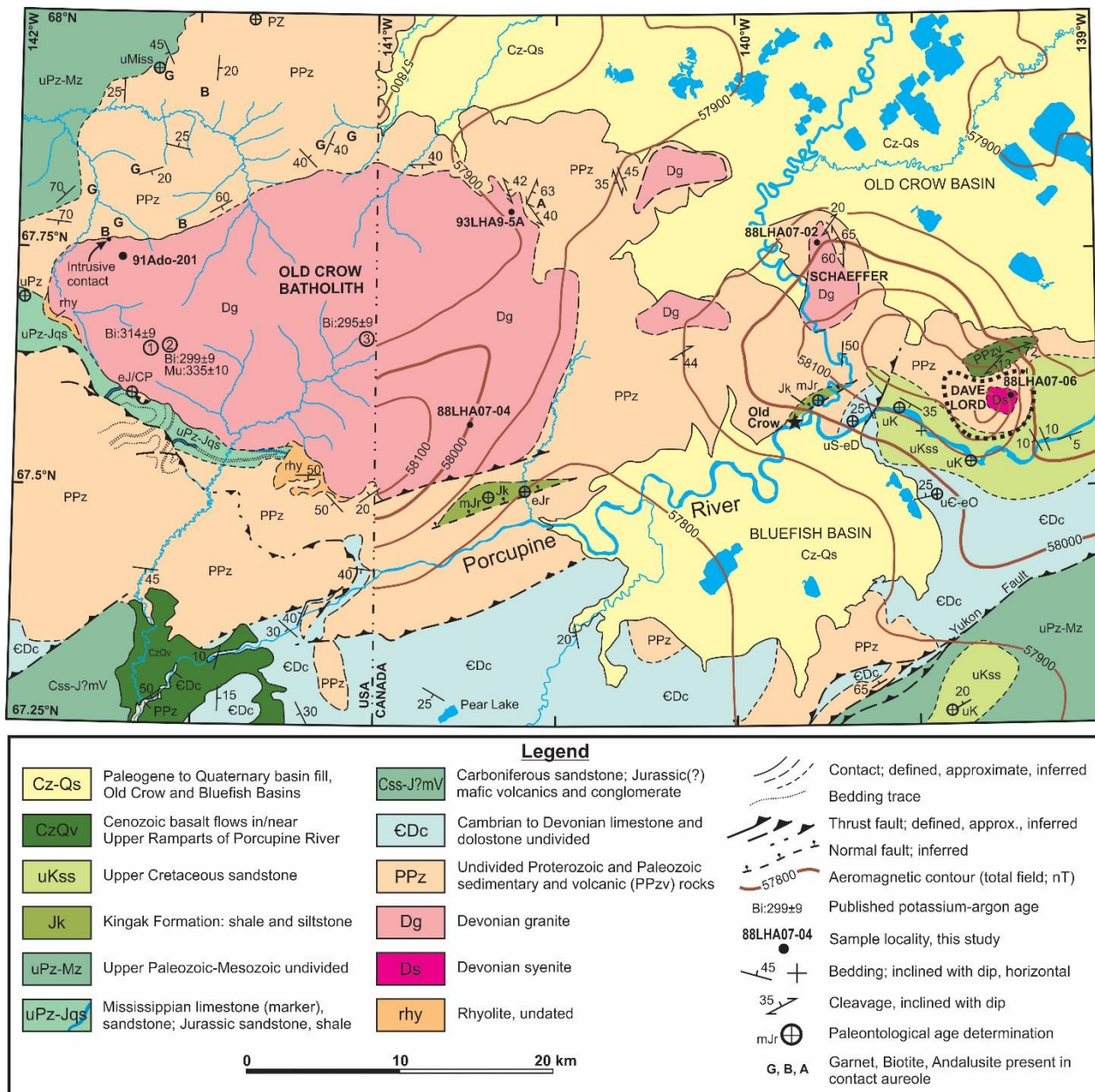


Figure 26. Regional location map for Old Crow, Schaeffer and Dave Lord intrusions is simplified from Norris (1981b), Brosgé and Reiser (1969), J. Dover, unpublished field compilation, and L.S. Lane, unpublished field compilations.

In Alaska, fossiliferous upper Paleozoic and Jurassic strata are mapped adjacent to the pluton (Reiser and Brosqué, 1969; Fig. 26); however, the nature of the contact, whether faulted or unconformable, is not defined. A normal fault is mapped along part of the southern margin of the batholith (Norris 1981b). This interpretation appears to reflect the rather linear trend of the granite's southernmost exposures, as well as outcrops of dated Jurassic strata in stream cuts nearby to the south.

Aeromagnetic total field contours in Yukon (Geological Survey of Canada, 1992) indicate a localized magnetic high, centred on the magnetite-bearing Dave Lord syenite felsenmeier field, whereas the much larger Old Crow granite and satellite exposures, lacking magnetite, have a more subdued magnetic signature. The heavy dashed outline around Dave Lord syenite suggests a possible extent for the pluton although it could also plausibly extend farther toward the northwest at depth. The subdued topography, widespread Cenozoic deposits and extensive vegetation cover limit the resolution of the compilation (Figs. 26, 27).

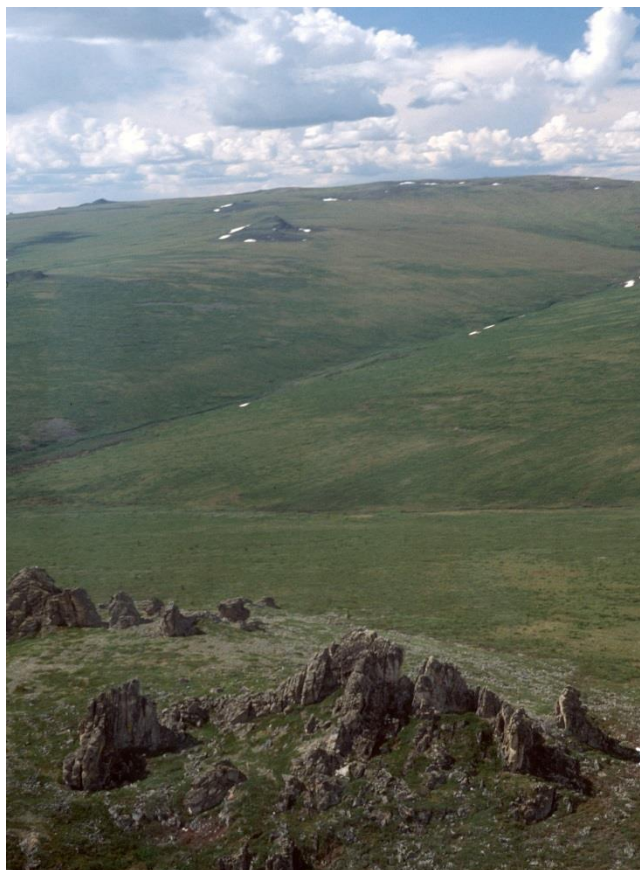


Figure 27. Locality 88LHA07-04 showing outcrop distribution and quality typical of the southeast part of Old Crow batholith (field photo 88-02-14). The lithology is a predominantly white, medium-grained granite with sparse K-feldspar megacrysts. Mafic phases comprise approximately 5%, dominantly biotite. Minor aplite veins are present. The outcrop is prominently jointed and also contains a locally developed fracture cleavage at 203/70°W.

This locality was sampled for U-Pb geochronology (Table B4, Sample 1: 367.5 ±1.2 Ma) and for geochemistry. This is also the locality reported on by Norris (1981b) with a K-Ar age of 265 Ma, sampled by G.C. Taylor in 1962.

Near the granite's northeastern margin, at geochemistry locality 93LHA9-5 (Fig. 28), included xenoliths (Fig. 29), and chlorite-sericite alteration (Fig. 30) document the incorporation of pre-existing crust and post-emplacement alteration, respectively.



Figure 28. Locality 93LHA9-5, granite tor near the northeast margin of Old Crow batholith. Here the lithology is a white megacrystic granite, weakly foliated, with cataastically deformed feldspar grains. A large aplite dike is also exposed here. (field photo 93-03-33)



Figure 29. Locality 93LHA9-5, outcrop surface showing abundant xenoliths up to 17 cm long, ranging from well rounded to angular. They include examples of felsic (aplitic), intermediate and mafic chemistry. These inclusions indicate that the granite has incorporated older lithologies during its emplacement, as implied by its complex chemistry (Lane and Mortensen, 2019). Abundant feldspar megacrysts are also visible. The pencil is approximately 15 cm long. (field photo 93-03-32)

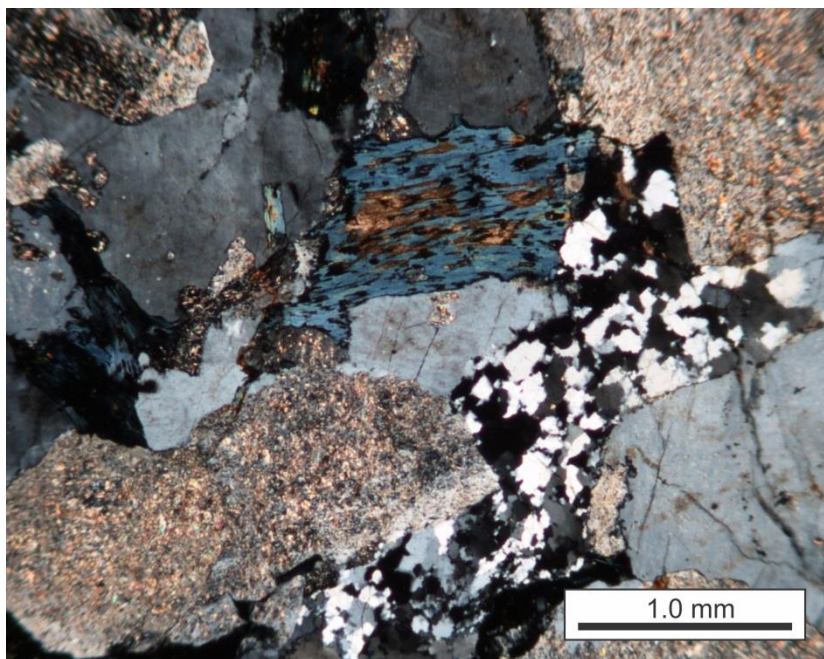


Figure 30. Old Crow granite, locality 93LHA9-5. Micrograph with crossed-polarizers. Advanced chlorite alteration and sericitization of the K-feldspars is evident. Quartz grains show extensive recrystallization.

Multiple occurrences of metamorphic biotite and garnet are reported in the vicinity of the northwest margin of the Old Crow batholith in Alaska, potentially indicating metamorphic conditions up to garnet zone (Brosgé and Reiser, 1969). Also, an exposed intrusive contact is mapped 2.5 km northwest from the site of geochronology sample 91Ado-201, near the pluton's northwestern margin (Fig. 26).

Relict andalusite, pseudomorphically replaced by sericite is documented adjacent to the northeast margin of Old Crow pluton (Fig. 31) indicating low pressure metamorphic conditions (Carmichael, 1978) consistent with epizonal emplacement conditions based on textural evidence (Burwash, 1997).

In a low pressure environment, the mapped presence of biotite and garnet adjacent to the northwest margin of the pluton (Fig. 26, see Brosgé and Reiser, 1969) would imply metamorphic temperatures above 400°C for biotite stability, and approaching 500°C for garnet (assuming an almandine composition).

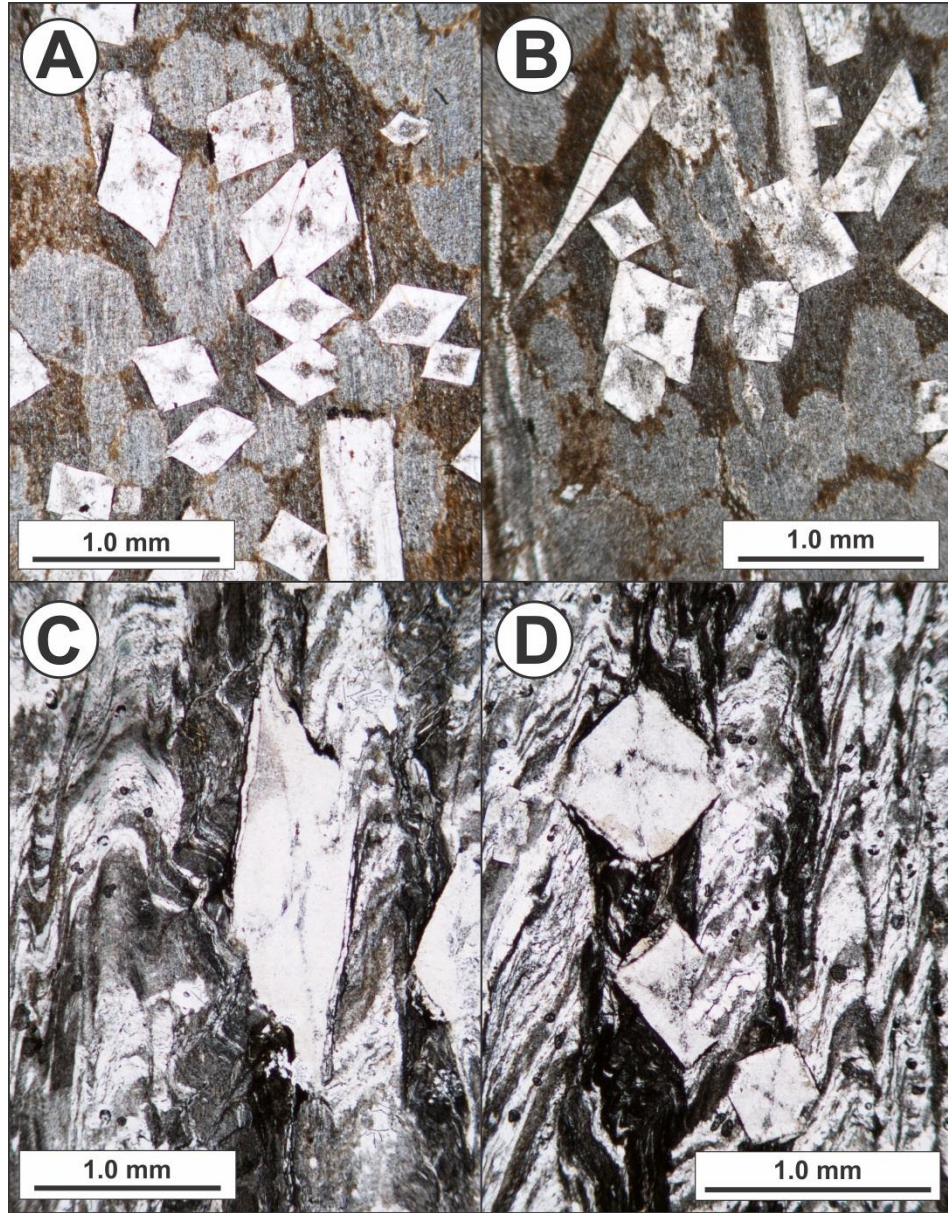


Figure 31. Locality 93LHA9-3, located approximately 400 m northeast of the Old Crow granite contact (at A on Figure 26). The most distal macroscopic porphyroblasts were observed approximately 600 m from the granite in this area. Thin section micrograph (A), in plane polarized light, shows anhedral albite (?) and euhedral chiastolitic andalusite, pseudomorphically replaced by sericite and locally fine muscovite, overgrowing a planar fabric. The presence of well-preserved fine silty laminae, just visible in image (B), indicates that the fabric is primary. Images (C) and (D) illustrate a post-intrusion crenulation cleavage accompanied by corrosion and possible distortion of the inclusion trains within the chiastolite. Images (A) and (B), from sample 9-3A; images (C) and (D) from sample 9-3D.

Schaeffer Granite

A well-developed contact aureole is present near the northern margin of Schaeffer granite. There it includes well-foliated albite-muscovite phyllite, calc-silicate and marble. Locally, granitic veins intrude the phyllite, cutting across the pre-existing foliation. The published regional map (Norris, 1981b) notes a bedding measurement dipping 60° west. Farther north along the margin, we recorded a local quartzite bedding attitude of $195/36^{\circ}$ W together with a tectonic fabric of $198/75^{\circ}$ W. Nearby, a foliation in the phyllite was measured at $215/20^{\circ}$ NW (see map, Fig. 26). This pink granitic phase (Fig. 32) may be one of several outlier exposures of the Old Crow batholith (see map, Fig. 26). Also at this locality, a granitic dyke cuts across the foliation in the metasediments.

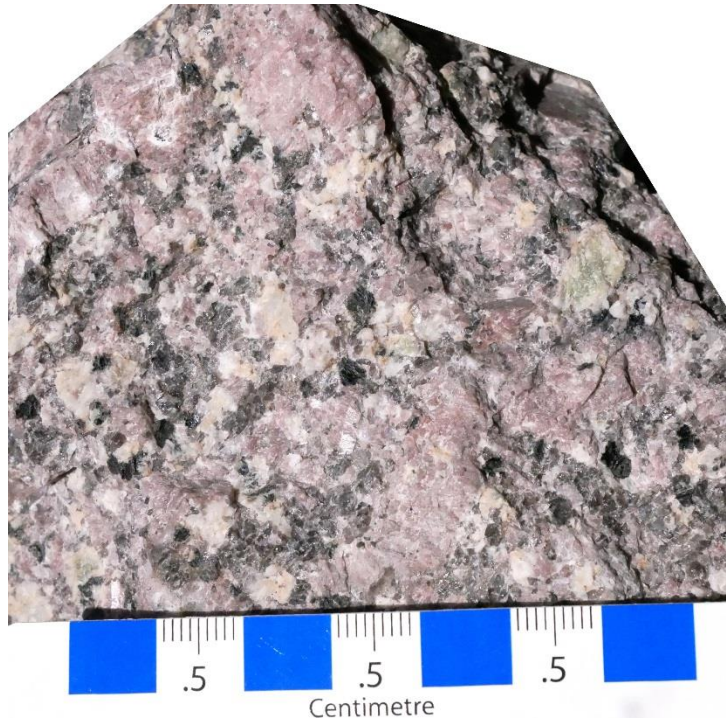


Figure 32. Schaeffer granite, locality 88LHA7-2. The coarse grained lithology is dominated by pink alkali feldspar, showing well developed perthitic texture in thin section; and lesser greenish plagioclase. In the field, we estimated ~70% feldspars, dominated by pink alkali feldspar, with ~25% quartz and ~5% mafics comprising biotite and hornblende in approximately equal amount. In thin section, minor greenish hornblende was observed, locally together with accessory opaque oxides, and locally altered to chlorite. Accessory tourmaline was observed in the field.

Dave Lord Syenite

Dave Lord pluton is a highly potassic syenite exposed only as boulder fields surrounded by Cenozoic sediments of the Old Crow Basin and its covering of sparse boreal vegetation. Accordingly, its extent and contact relationships are not defined.

The nearest bedrock outcrops comprise undeformed to locally well-foliated mafic metavolcanic rocks of uncertain age, exposed 2-5 km northeast of the syenite; and Upper Cretaceous, marine sandstones predominantly exposed along Porcupine River south and west of the pluton (Fig. 26).

Although no outcrop exposures of Dave Lord syenite exist, the two extensive felsenmeer fields provide a wide variety of colours and textures. Pink phases dominated by potassic feldspars appear to dominate (Figs. 33 to 35). However, light to dark grey phases are also present (Figs. 36 and 37).

Dave Lord pluton is spatially associated with a significant aeromagnetic anomaly, providing an indication of its shallow subsurface extent (Fig. 26). Magnetite is a prominent accessory mineral (Fig. 38) that in hand sample elicits a response from a pencil magnet. This magnetic signature, together with the absence of continental glaciation in the basin, rules out the possibility that the blocks exposed as felsenmeer were transported from elsewhere.



Figure 33. Pink syenite, locality 998NC (the same locality as geochronology sample 88LHA07-06). Scale is in cm and mm.



Figure 34. Pink syenite, locality 998NC; cut surface, showing clots of hornblende and an unidentified rounded inclusion. Scale is in cm and mm.



Figure 35. Slightly weathered pink, coarse grained syenite, locality 1259NC (approx. 1 km west of 998NC). The dominant mineral phase is alkali feldspar.

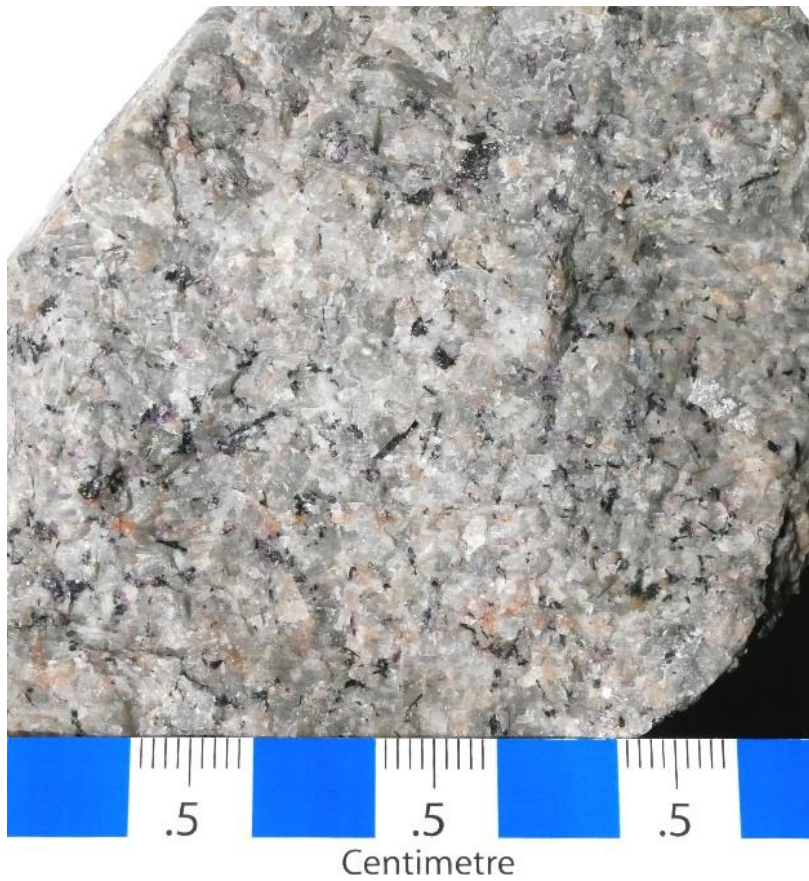


Figure 36. (at left) Grey variety of the Dave Lord syenite, locality 998NC. Coarse grainsize and elongate hornblende grains are notable.

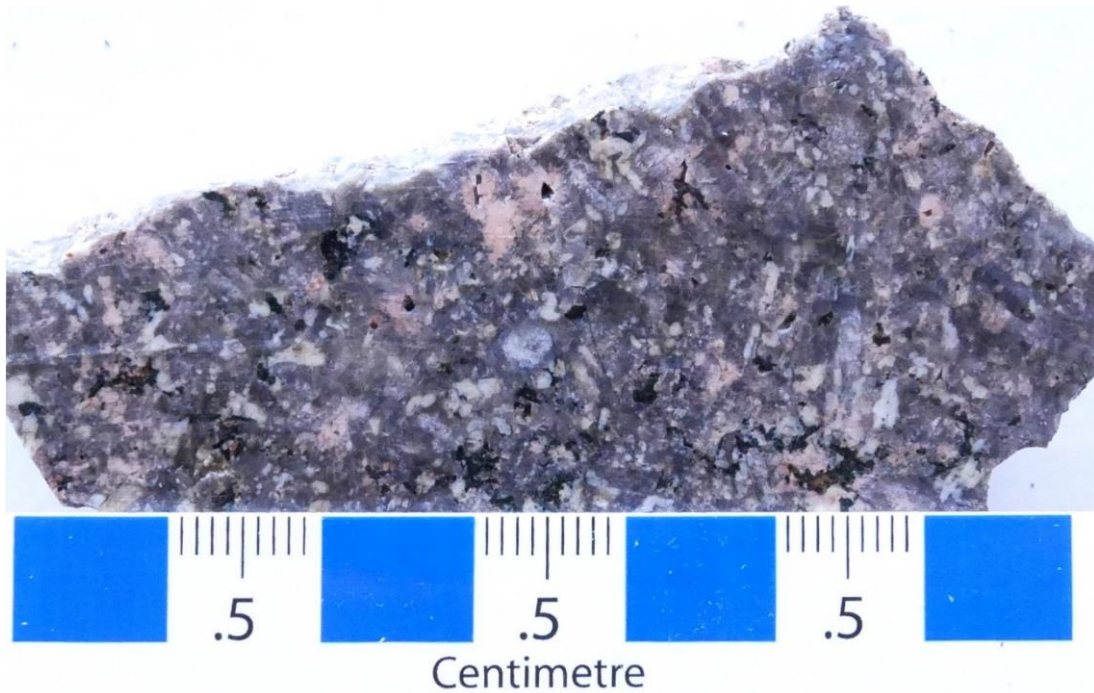


Figure 37. (below) Cut surface from geochronology sample 88LHA7-6 (see map, Fig. 26). Pink alteration of feldspar is visible adjacent to small vugs in the sample.

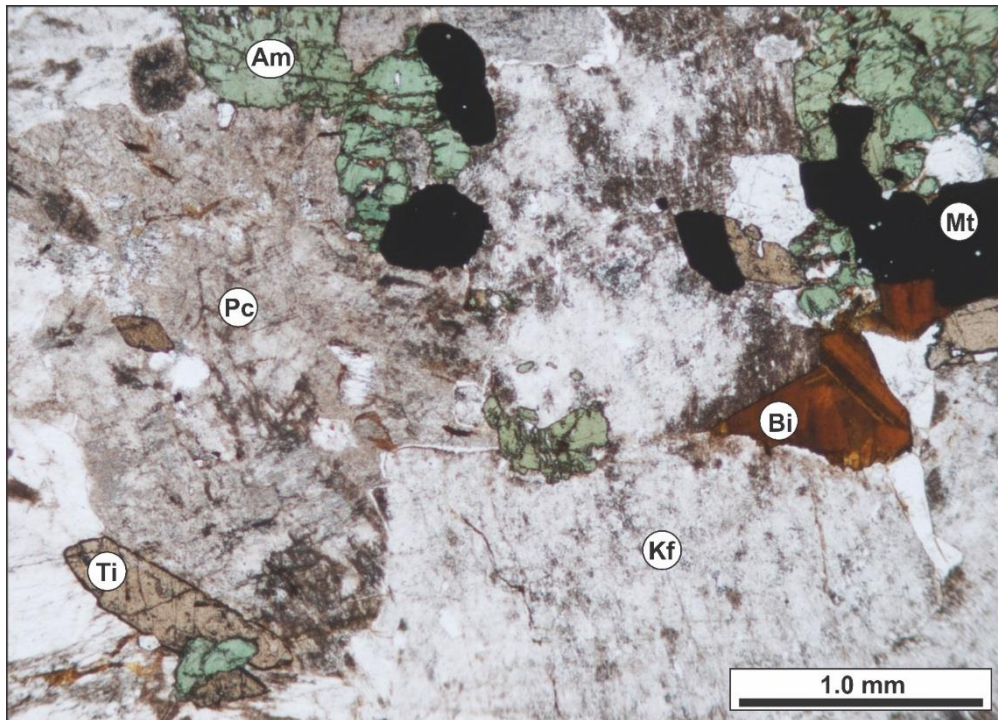


Figure 38. Dave Lord syenite microphotomosaics: plane polarized light (top), crossed-nicols (bottom). Both images cover a similar area. The rounded magnetite (Mt) grain, top-centre in the upper photo, is the labelled grain at the left of the lower photo. Geochronology sample 88LHA7-6. Light mineral grains are dominated by K-feldspar (Kf), with minor, highly altered plagioclase (Pc), locally preserving albite twinning. Also shown are biotite (Bi), and titanite (Ti). Nepheline is not observed in this thin section.

Bear Mountain Syenite

The Bear Mountain pluton in easternmost Alaska (Figs. 1, 39), exposed in the Table Mountain map area (Brosgé et al., 1976), is mapped as two adjacent exposures of potassic syenite (Fig. 40), with an additional small outlier of quartz-feldspar porphyry (Fig. 41) farther west. The western exposure is in contact with three map units, comprising sandstone, grey phyllite and greenstone (Paleozoic) and Devonian to Mississippian Kanayut or Kekiktuk (MDK) successions. The larger, eastern exposure also is shown in contact with map unit MDK, as well as Mississippian siltstone of the Kayak Formation and limestone of the Lisburne Group. Exposures of Kayak and Lisburne strata are mapped as overlying (or projecting into) the intrusion. The pluton is inferred to truncate a thrust fault juxtaposing unit MDK against Lisburne (north of locality 91-288), whereas a second fault juxtaposes the Kayak Formation against the pluton (Brosgé et al., 1976).

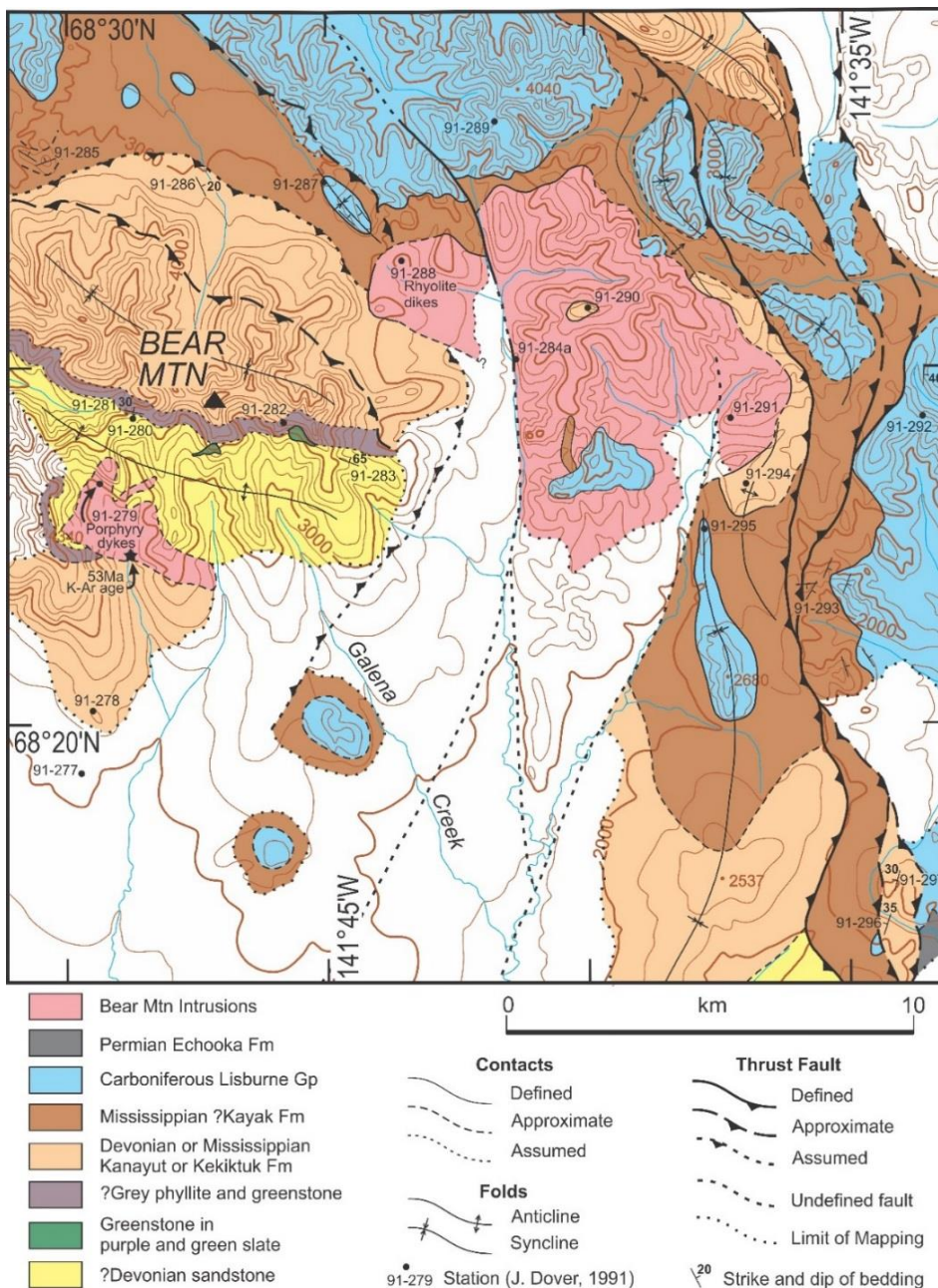


Figure 39. Bear mountain location map showing the sampled field control points (91-279 and 91-284a), compiled from Brosgé et al. (1976) and unpublished field mapping in 1991 by J. Dover. K-Ar age is from Barker and Swainbank (1986).

Figure 40. Cut surface of Bear Mountain rhyolite, sample 91-284a, dominated by highly altered K-feldspar.

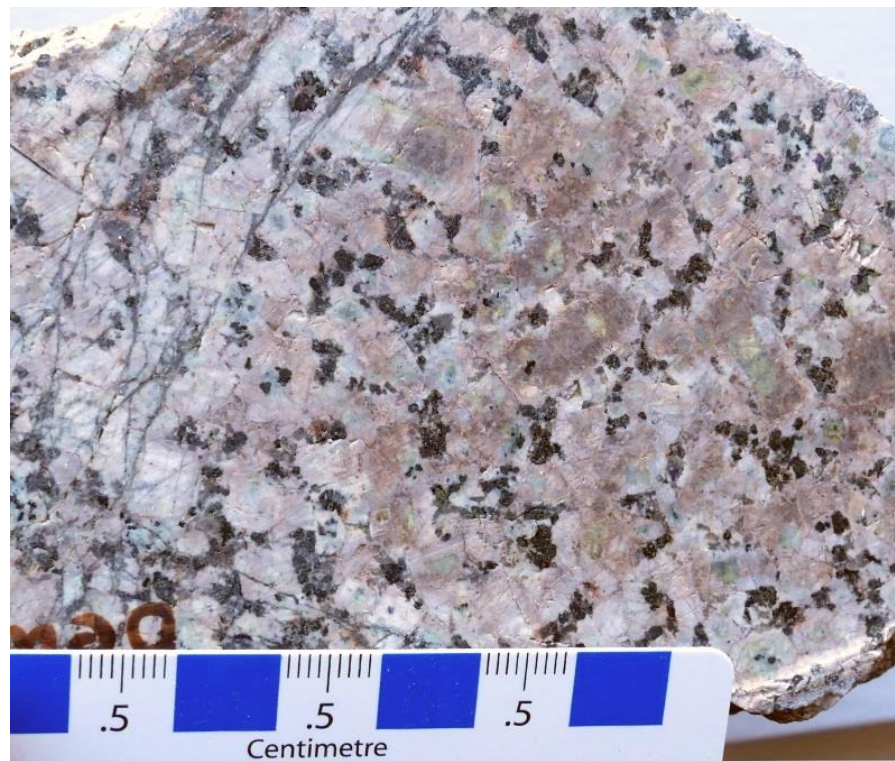
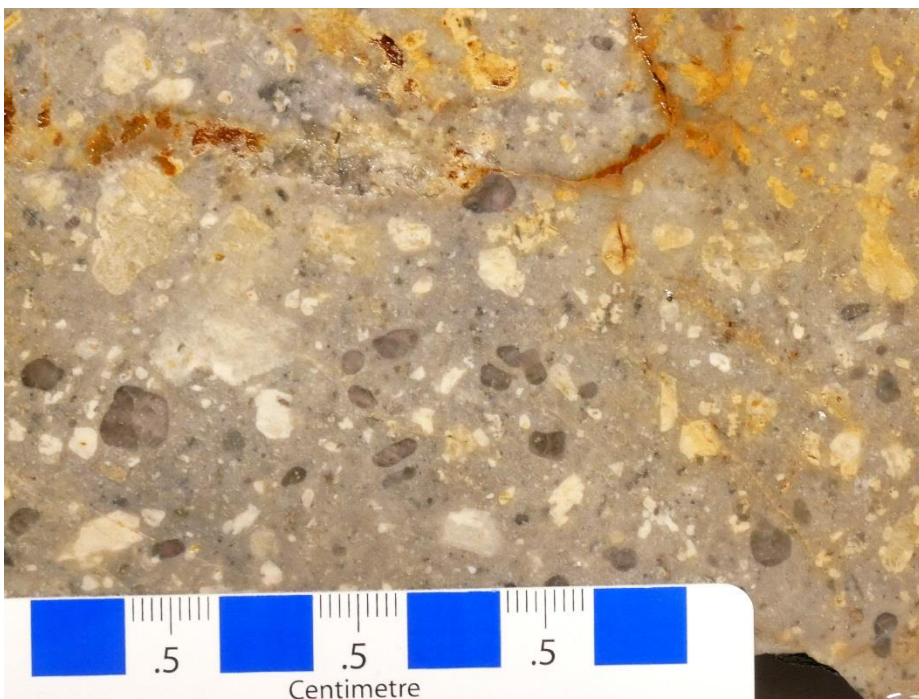


Figure 41. Cut surface of the quartz-feldspar porphyry, sample 91-279. Large rounded quartz and feldspar grains are abundant, in a pale grey aphanitic groundmass.



CORRELATIONS WITH REGIONAL AEROMAGNETIC DATA

The plutons of northern Yukon are restricted to the area enclosed by the British, Barn and Keele ranges, which is largely underlain by Paleozoic and Proterozoic strata. Sedgwick, Hoidahl and Fitton plutons are distributed toward the northeast and their contacts are relatively well exposed. In contrast, Ammerman, Dave Lord, Schaeffer and Old Crow plutons are within or adjacent to the Cenozoic Old Crow Basin and their contacts are only locally exposed, if at all. Within the study area, available aeromagnetic coverage, at line spacings of 2-3, km is too coarse to permit a detailed correlation to the bedrock geology. However, the upper crustal magnetic response is generally somewhat greater where the Mesozoic and younger successions are thin or absent (Fig. 42). Of the suite of mapped plutons, only Sedgwick and Dave Lord are reported to contain accessory magnetite (Burwash, 1997). Accordingly, a significant magnetic response might not be expected in most cases. Although most of the plutons are spatially associated with modest, regional magnetic highs, these responses do not in general correspond with the mapped outlines

of the plutons (Fig. 42). The exception is Sedgwick granite which has well exposed contacts that correspond closely to a local magnetic high that is superimposed on the broader regional feature. In particular, the first vertical derivative anomaly aligns closely with the east and west contacts of the pluton (Fig. 43).

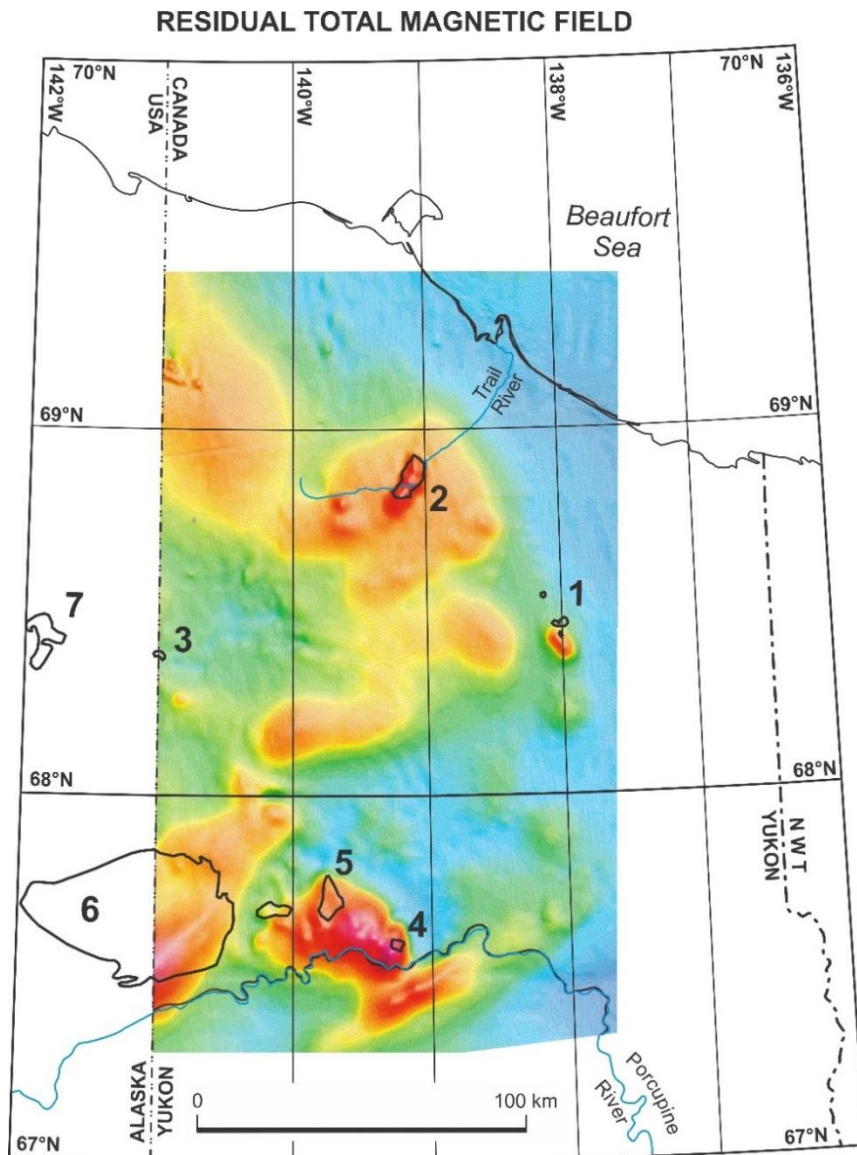


Figure 42. Pluton outlines plotted on the residual total magnetic field (Miles and Oneschuk, 1999). Two localized highs underlie the region. One corresponds with the Sedgwick pluton (2), and the other occurs in the vicinity of Dave Lord (4) and Schaeffer (5) plutons.

The other magnetite-bearing pluton, Dave Lord syenite, is exposed only as felsenmeer distributed across a hillside, some 25 km east of the town of Old Crow (Fig. 26). It is spatially associated with a magnetic high that extends to the northwest toward Schaeffer granite (Fig. 42). The intensity of this high relative to the adjacent magnetically quiescent area is noteworthy. Scattered outcrops across the area indicate widespread early Paleozoic and Proterozoic carbonate and clastic strata and mafic volcanic rocks locally overlain by a thin veneer of Late Cretaceous sandstone (Fig. 26). Aside from the adjacent mafic volcanic rocks that undoubtedly contribute to the magnetic response, it is uncertain how the intensity of this magnetic high may reflect the near surface and/or subsurface extent of the syenite, as opposed to the older sedimentary rocks widely exposed toward the west and northwest toward Old Crow batholith. One estimate of the pluton's possible near-surface extent is shown in Fig. 26. It could plausibly extend much farther to the northwest in the subsurface. However, a definitive answer would require a modelling study based on a determination of the magnetic susceptibilities of the units. The continuity of this magnetic anomaly was previously cited as one of multiple arguments refuting the hypothetical extension of the Alaskan Kaltag Fault into Yukon (Lane, 1992).

FIRST VERTICAL DERIVATIVE OF MAGNETIC ANOMALIES

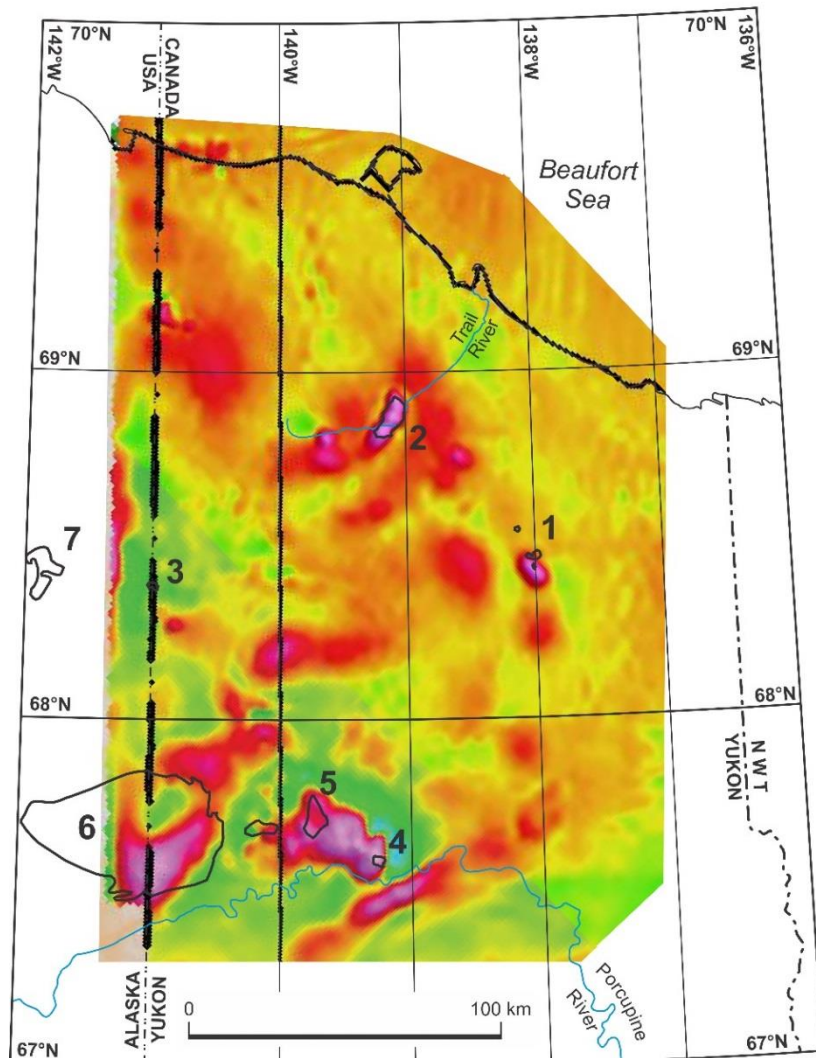


Figure 43. Yukon pluton outlines plotted on magnetic first vertical derivative map (Miles and Oneschuk, 2016). The contacts of Sedgwick pluton (2) correspond closely to the magnetic response. In the vicinity of Dave Lord (4) and Schaeffer (5) plutons, the magnetic response is much larger than the exposed extent of the magnetite- bearing Dave Lord pluton, suggesting that the pluton may have a much larger shallow subsurface extent.

GEOCHEMISTRY

Geochemistry data are presented in Appendix Tables B2 and B3. Table B2a summarizes the major and trace element data for all of the plutons in this study, together with the data presented in Burwash (1997). Tables B2b and B2c provide an earlier set of chemistry data analysed in-house during 1993-94. In contrast to the coeval granites, the Dave Lord syenite preserves a within-plate chemistry, whereas the granites cluster near the junction of the syn-collisional, volcanic arc and within-plate fields (Fig. 44).

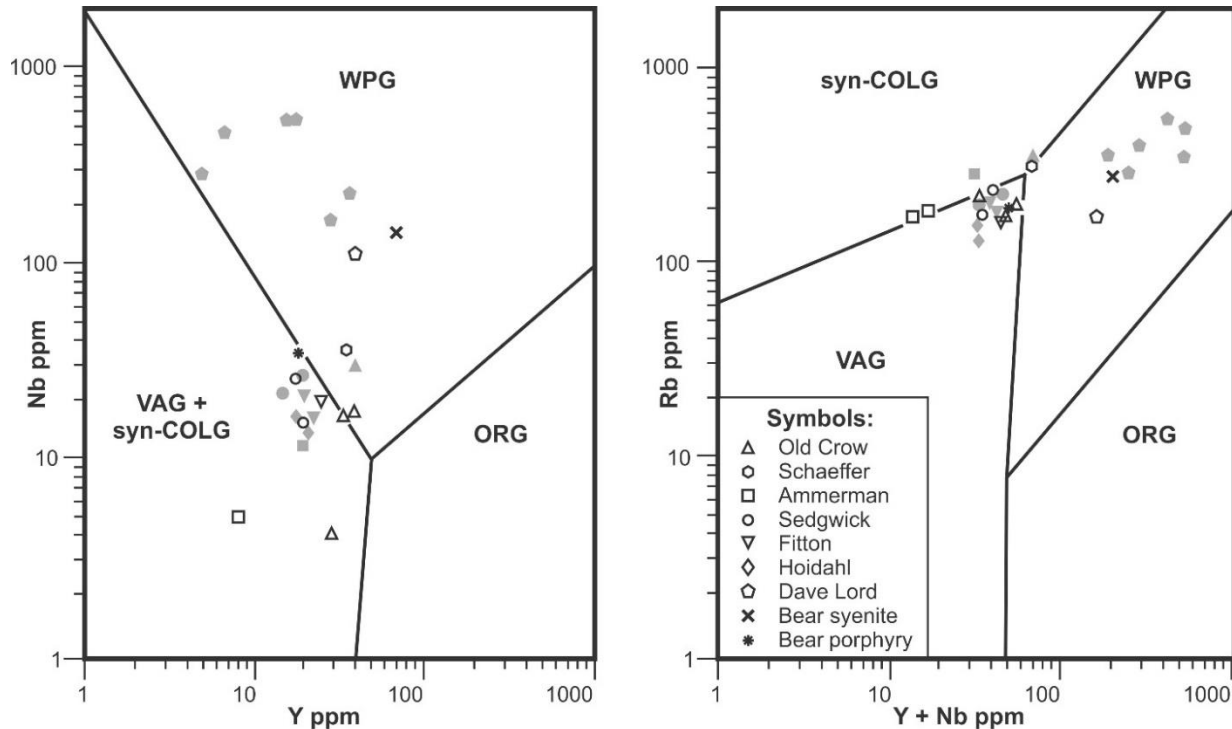


Figure 44. Trace element tectonic discrimination plots (Pearce et al., 1984). Our data are plotted as open black symbols superimposed on shaded symbols from Burwash (1997). Both data sets show distributions consistent with a mantle-derived within-plate setting for the syenites and a more complex evolution for the granites, see Lane and Mortensen (2019) for an in-depth interpretation of a full suite of discrimination plots.

In addition all existing Rb-Sr and Nd-Sm isotopic and geochemical data are tabulated for the plutons (Appendix Table B3a), as well as Nd-Sm data for a selection of Proterozoic and Paleozoic strata (Appendix Table B3b). Their initial $\text{Sr}^{87}/\text{Sr}^{86}$ ratios and ε_{Nd} values provide additional support for significant crustal input into the granitic magmas (see Lane and Mortensen, 2019).

Figure 45 shows the ε_{Nd} values for the granites and for examples of the enclosing country rocks, calculated at 370 Ma, the approximate age of the intrusions. This is done because ε_{Nd} values change with time due to the radioactive decay of Sm. Plotting all results for this age allows for a better evaluation of the sedimentary rocks as potential source material and/or contaminant to the plutonic rocks by comparing ε_{Nd} values at the time of intrusion.

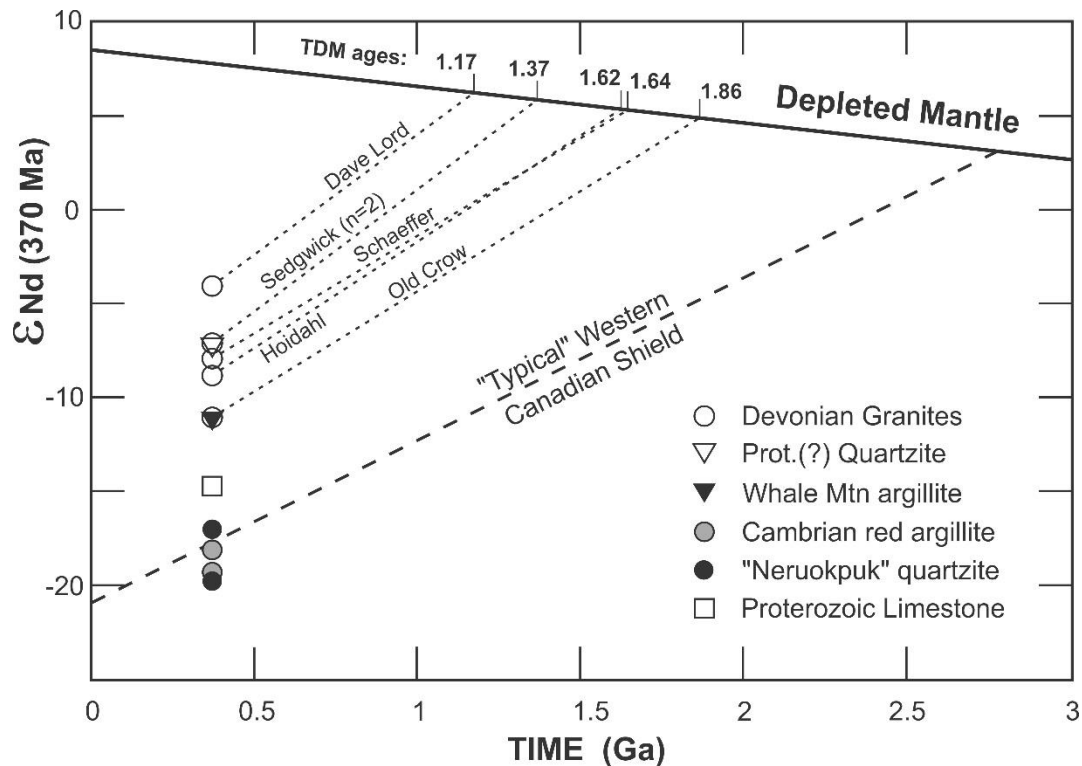


Figure 45. Sm-Nd geochemistry plotted as ε_{Nd} vs Time, with TDM (Depleted Mantle Model) ages, for five of the Devonian plutons, and a suite of enclosing metasedimentary rock units (Table B3). The depleted mantle curve is from DePaolo (1981). The “Typical Western Canadian Shield” curve represents a generalized reference line that typifies the western Canadian Shield and is not meant to indicate a specific dataset (Thériault, 1992; see also Davis and Hegner, 1992; Cousens, 2000).

The “Neruokpuk” quartzites, Cambrian argillites, Proterozoic limestone and Whale Mountain argillite were clearly derived from Early Proterozoic source rocks as suggested by their 2.0 to 2.6 Ga model ages (Table B3b). Also, the negative $\varepsilon_{\text{Nd}}(370 \text{ Ma})$ values of these rocks (-11 to -20) are more negative than the -4 to -11 values from the plutonic rocks. Although incorporation of the “Neruokpuk” and Cambrian rocks into the magmas is not precluded, it is clear that these (and isotopically similar) rocks are not the only source to the granitoids and that a more juvenile source, such as mixing with juvenile mantle-derived melts, must be invoked.

The unnamed Proterozoic(?) quartzite is clearly different from the other sediments. The ϵ_{Nd} (370 Ma) value of -7.3 for this sample falls in the range of the Devonian plutons, as does its 1.78 Ga model age. Although mapped as a Proterozoic unit, the age of this unit is speculative and a younger age is equally possible. Unlike typical Neoproterozoic and Cambrian quartzites in the region, this is a clean quartz-feldspar arenite with quartz grains that are recrystallized and uniform in size, and with minor (~5%) feldspar grains and accessory secondary sericite. It could be derived from a much more juvenile source, like the granites; or more plausibly, it could be derived largely from the adjacent Schaeffer granite.

Several conclusions may be drawn from these data:

1. The plutonic rocks are derived largely from pre-existing crust. This is suggested by the negative ϵ_{Nd} values. Light Rare Earth Element (LREE)-enriched rocks (e.g. continental crust) acquire negative ϵ_{Nd} values with time, as opposed to positive values which are typical of LREE-depleted mantle. Continental crust that has been recently derived from mantle melting typically displays positive ϵ_{Nd} values, similar to its mantle source. Thus the negative ϵ_{Nd} of the granites show that they were probably derived from long-lived continental crust.
2. The ϵ_{Nd} values of the granites may represent mixing between mantle-derived material with positive ϵ_{Nd} and older sedimentary material (by assimilation at shallow levels in the crust?) such as the Neoproterozoic and Cambrian sedimentary units in the vicinity. In such a case, the ϵ_{Nd} values of the granites would be intermediate between positive values from the mantle end-member and strongly negative values from the Neoproterozoic and Cambrian sediments.
3. If the granites are derived solely by melting of the crust, the granites would have the same ϵ_{Nd} values as their crustal source(s). On this basis the Neoproterozoic and Cambrian rocks can be ruled out as the sole source of the magmas.
4. Neoproterozoic and Cambrian sediments have Nd isotopic compositions that are consistent with derivation from the western Canadian Shield. The typical evolution curve for the western Canadian Shield line shown in Figure 45 is a reference line only, illustrative of the western Shield. However, the Nd isotopic composition of individual rock units in the western Canadian Shield is highly variable.
5. The Nd isotopic composition of the Whale Mountain argillite and limestone indicates that they are clearly more juvenile than average western Canadian Shield rocks.

GEOCHRONOLOGY

U-Pb Geochronology

Various attempts at isotopic dating of the north Yukon plutons have taken place since the early reconnaissance of the region (e.g., Baadsgaard et al., 1961; Wanless et al., 1965, 1974; reviewed in Burwash, 1997). The uranium-lead geochronology data for this study were acquired over a number of years (Lane et al., 1993), beginning with a suite of multi-grain TIMS (thermal ionization mass spectrometry) analyses carried out at the Geological Survey's Geochronology lab, followed up later by additional TIMS analyses at the Pacific Centre for Isotopic and Geochemical Research at the University of British Columbia (PCIGR). These data are presented in Appendix Table B4. Substantial scatter in the analytical data from each sample, interpreted as due to variable amounts of inheritance, combined with significant post-crystallization lead-loss, made it impossible to generate defendable crystallization ages for most of the samples. Accordingly, zircon samples were later re-analysed using laser-ablation inductively coupled plasma mass spectroscopy (LA) at PCIGR, which are presented below in Appendix Table B5. See Lane and Mortensen (2019) for a concise summary of the methodology employed in this study.

Interpretation of time-resolved laser ablation signals from line scans, as was employed in this study, makes it possible to extract data from portions of a single zircon that have not been affected by post-crystallization Pb-loss, and to avoid any parts of the signal that might be from inherited cores or altered and disturbed zircon, and thus give a true age for the “igneous” zircon. Individual analyses are therefore accurate but have relatively low precision, so typically, a large number of such analyses are pooled to produce a weighted average age (usually the $^{206}\text{Pb}/^{238}\text{U}$ ages for Phanerozoic zircons, since these are the most precisely determined calculated ages).

The presence of zircon grains that are substantially older than the interpreted crystallization age of a pluton are most reasonably interpreted to represent either inherited cores or xenocrysts. Zircons that give ages that are only slightly older than the main cluster of igneous ages, however, must be derived either from very young clastic or volcanic rocks in the subsurface (only slightly older than the intrusion itself), or more probably from early phases of intrusion that are not exposed at the present erosional level. Magmatism in any area rarely occurs in only one very brief pulse, and intrusions of batholithic extent are commonly emplaced over many millions of years, so we consider it quite reasonable to suggest that this has happened in the study area. If correct, then the ages that we have obtained for the intrusions as exposed at the present erosional level may indeed have been emplaced through slightly older components of the same overall magmatic “event”. The presence of xenocrystic zircon is almost ubiquitous in felsic intrusions in the upper crust, and crustally derived magmas almost invariably include inherited zircon cores (if they are the product of melting of zircon-bearing source rocks). The original crystallization age of a zircon xenocryst will be retained after incorporation into a felsic magma – such magmas are typically relatively low temperature (<1000 degrees), and it would take much higher temperatures than this to completely reset the zircon systematics. The exception to the common presence of xenocrystic zircons in felsic igneous rocks is in alkaline magmas, such as Dave Lord or Bear Mountain, which usually have a very high Zr solubility, and therefore inherited zircons, or xenocrystic zircon incorporated into the magma at a relatively early stage, will typically be completely dissolved before the magma finally crystallizes.

Rubidium-Strontium Analyses ca. 1984-85

In the mid-1980's, the Earth Physics Branch of the (then) Ministry of Energy Mines and Resources Canada undertook a regional sampling project for uranium, potassium and thorium in the northern Yukon plutons, as part of a research program to study regional heat flow patterns in northern Canada. Within that context, two Rb-Sr geochronology contracts were awarded to Carleton University to assess the ages and possible magma sources of the plutons. In particular, if the granites could be shown to be derived from a crustal source, it would have significant implications for region's tectonic evolution (A. Judge, written communication, 1988).

We include, as Appendix A, summaries of two unpublished Rb-Sr geochronology reports from the mid-1980s, produced by Drs. Keith Bell and John Blenkinsop of Carleton University, Ottawa (Bell and Blenkinsop, 1984, 1985). Although these data are not current, they form an important step in the process of understanding the geological evolution of the plutons and their surroundings.

The initial contract (Bell and Blenkinsop, 1984) consisted of a literature review of published isotopic studies in the region (not summarized), and a preliminary analysis of one sample, in five splits, from Old Crow batholith. The second contract (Bell and Blenkinsop, 1985) analysed 48 samples collected in 1984 from six intrusions to determine their Rb/Sr ages and to assess possible recycling of continental crust using their initial $^{87}\text{Sr}/^{86}\text{Sr}$ ratios.

ACKNOWLEDGEMENTS

The authors appreciate constructive comments from critical reviewer, G.S. Stockmal.

REFERENCES

- Baadsgaard, H., Folinsbee, R.E. and Lipson, J., 1961. Caledonian or Acadian granites of the Northern Yukon Territory. In *Geology of the Arctic*. Edited by G.O. Raasch. Proceedings of the 1st International Symposium on Arctic Geology, Vol. 1. Alberta Society of Petroleum Geologists, Calgary, AB. pp. 458-465.
- Batchelor, R.A., and Bowden, P., 1985. Petrogenetic interpretation of granitoid rock series using multicationic parameters. *Chemical Geology*, v. 48, p. 43-55.
- Bell, K. and Blenkinsop, J., 1984. Geochronology and Isotopic Studies of Granitoid Rocks from the Northern Yukon – Final Report. Unpublished contractor's report, Earth Physics Branch, Department of Energy Mines and Resources Canada. 14p.
- Bell, K. and Blenkinsop, J., 1985. Yukon Geochronological Project, 1984-1985 Final Report. Unpublished contractor's report, Earth Physics Branch, Department of Energy Mines and Resources Canada. 12p.
- Brosgé, W.P., and Reiser, H.N., 1969. Preliminary geologic map of the Colleen Quadrangle, Alaska. U.S. Geological Survey. Open File 69-0025 (formerly OF 370), 1 sheet, scale 1:250,000.

Brosgé, W.P., Reiser, H.N., Dutro, J.T., Jr. and Detterman, R.L. 1976. Reconnaissance geologic map of the Table Mountain quadrangle, Alaska. U.S. Geological Survey. Open File Map 76-546, 2 sheets, 1:200,000 scale.

Burwash, R.A., 1997. Petrology of the Northern Yukon Intrusive Suite. In The Geology, Mineral and Hydrocarbon Potential of Northern Yukon Territory and Northwestern District of Mackenzie. Edited by D.K. Norris. Geological Survey of Canada, Bulletin 422, p. 359-367.

Carmichael, D. M., 1978. Metamorphic bathozones and bathograds; a measure of the depth of post-metamorphic uplift and erosion on the regional scale. American Journal of Science. v. 278, p. 769-797; doi:10.2475/ajs.278.6.769

Cecile, M.P., and Lane, L.S., 1991. Geology of the Barn Uplift. Geological Survey of Canada Open File 2342, 1 sheet, 1:50,000 scale.

Cousens, B.L., 2000. Geochemistry of the Archean Kam Group, Yellowknife Greenstone Belt, Slave Province, Canada.

Davis, W.J., and Hegner, E., 1992. Neodymium isotopic evidence for the tectonic assembly of late Archean crust in the Slave Province, northwest Canada. Contributions to Mineralogy and Petrology, v. 111, p. 493-504.

DePaolo, D.J., 1981. Neodymium isotopes in the Colorado Front Range and crust-mantle evolution in the Proterozoic; Nature, v. 291, p. 193-196.

Findlay, D.C., and Caine, T.W. 1981. Assessment of the mineral and fuel resource potential of the proposed northern Yukon national park and adjacent areas (Phase 1); Geological Survey of Canada Open File 760, 31p.

Geological Survey of Canada, 1992. Aeromagnetic total field, Old Crow, Yukon Territory; Geological Survey of Canada, Map 7931G, scale 1:250,000.

Lane, L. S., 1991. The Pre-Mississippian "Neruokpuk Formation", northeastern Alaska and northwestern Yukon: review and new regional correlation. Canadian Journal of Earth Sciences, v. 28, p. 1521-1533, doi: 10.1139/e91-136.

Lane, L.S., 1992. Kaltag Fault, northern Yukon: Constraints on evolution of Arctic Alaska. Geology, v. 20, p. 653-656.

Lane, L.S., 1998. Late Cretaceous-Tertiary tectonic evolution of northern Yukon and adjacent Arctic Alaska. American Association of Petroleum Geologists Bulletin, v. 82, p. 1353-1371.

Lane, L.S., and Mortensen, J.K., 2019. U-Pb geochronology, Nd-Sm geochemistry, structural setting and tectonic significance of Late Devonian and Paleogene intrusions in northern Yukon and northeastern Alaska. Canadian Journal of Earth Sciences, v. 56, in press, doi: 10.1139/cjes-2018-0131

Lane, L.S., Mortensen, J.K., and Theriault, R.J., 1993. Tectonic setting, U-Pb geochronology and geochemistry of Late Devonian plutons, northern Yukon. Geological Association of Canada, Mineralogical Association of Canada, Joint Annual Meeting, Edmonton, Alberta, May 1993, Abstracts with Program, v. 18, p. A55.

Miles, W., and Oneschuk, D., 1999. Residual total magnetic field, Yukon Territory. Geological Survey of Canada Open File 3740, scale 1:1,500,000.

Miles, W., and Oneschuk, D., 2016. First vertical derivative of magnetic anomalies map, Canada / Carte des anomalies de la dérivée première verticale du champ magnétique, Canada. Geological Survey of Canada Open file 7878, scale 1:7,500,000, <https://doi.org/10.4095/297338>

Norris, D.K., 1981a. Geology, Blow River and Davidson Mountains, Yukon Territory and District of Mackenzie, Geological Survey of Canada Map 1516A, 1 sheet, 1:250,000 scale.

Norris, D.K., 1981b. Geology, Old Crow, Yukon Territory, Geological Survey of Canada Map 1518A, 1 sheet, 1:250,000 scale.

Norris, D.K., 1981c. Geology, Bell River, Yukon Territory and District of Mackenzie, Geological Survey of Canada Map 1519A, 1 sheet, 1:250,000 scale.

Norris, D.K. 1984. Geology of the northern Yukon and northwestern District of Mackenzie. Geological Survey of Canada. Map 1581A. <https://doi.org/10.4095/120537>.

Norrish, K. and Chappell, B.W., 1967. X-ray fluorescence spectrography. In: Zussman, J. (ed.) Physical Methods in Determinative Mineralogy, London and New York, Academic Press, p. 161-214.

Pearce, J.A., Harris, N.B.W., and Tindle, A.G., 1984. Trace element discrimination diagrams for the tectonic interpretation of granitic rocks. Journal of Petrology, v. 25, 956-983, <https://doi.org/10.1093/petrology/25.4.956>

Thériault, R.J., 1992. Nd Isotopic Evolution of the Taltson Magmatic Zone, Northwest Territories, Canada: Insights into Early Proterozoic Accretion along the Western Margin of the Churchill Province. Journal of Geology, v. 100, p. 465-475.

Wanless, R.K., Stevens, R.D., Lachance, G.R., and Dilabio, R.N., 1974. Age determinations and geological studies, Report 12. Geological Survey of Canada Paper 74-2, 72p.

Wanless, R.K., Stevens, R.D., Lachance, G.R. and Rimsaite, R.Y.H., 1965. Age determinations and geological studies, Part 1 – isotopic ages, Report 5. Geological Survey of Canada, Paper 64-17, 126 p.

Appendix A:
**Part 1: Summary of “Geochronology and Isotopic Studies of Granitoid Rocks
from the Northern Yukon – Final Report”**

K. Bell and J. Blenkinsop

(Figures and Tables numbered as in original report.)

In the initial (1984) study, one sample from Old Crow batholith provided by Earth Physics Branch was assessed to be suitable for Rb-Sr isotopic analysis. It was divided into five splits (OCB-A to OCB-E) and each was processed separately. If variations in the $^{87}\text{Sr}/^{86}\text{Sr}$ ratio could be resolved across the five splits, a whole rock isochron would be possible. Ultimately, the isotopic ratios of the splits were determined to be too uniform to produce an isochron (Table 2).

The Rb and Sr abundances were measured in duplicate by X-ray fluorescence using a method where the mass absorption coefficients are determined directly, using a Finnigan MAT261 mass spectrometer. Two of the splits (OCB-A and OCB-D) were further processed for biotite and feldspar mineral separations, according to the following procedure:

- Crushing to -40 / +80 mesh;
- Washing in de-ionized water;
- Separation into magnetic and non-magnetic fractions on an isodynamic separator;
- Biotite, almost 98% pure, was picked from both splits;
- ~200 mg of mixed feldspar was hand picked from OCB-D;
- From OCB-A, the non-magnetic fraction was separated into light and heavy parts using methyl iodide diluted with acetone to a specific gravity of 1.75-1.81 and ~300 mg was obtained from the heavy fraction;
- ~200 mg of feldspar was hand picked from the light fraction
- the mineral separates thus obtained were spiked with a ^{87}Rb - and ^{84}Sr -enriched spike.

Table 2: Isotopic Data

<u>Sample</u>		<u>Rb</u> <u>(ppm)</u>	<u>Sr</u> <u>(ppm)</u>	<u>$^{87}\text{Rb}/^{86}\text{Sr}$</u> <u>(atomic)</u>	<u>$^{87}\text{Sr}/^{86}\text{Sr}$</u> <u>(atomic)</u>
OCB-A	feldspar (light)	263	420	1.82	0.73749
OCB-A	feldspar (heavy)	128	506	0.735	0.73306
OCB-A	biotite	542	28.9	55.3	0.94066
OCB-D	feldspar (mixed)	237	394	1.74	0.73698
OCB-D	biotite (a)	593	17.1	106	1.2820
	biotite (b)	748	22.1	102	1.1979
OCB-A	w.r.	240	206	3.38	0.74408
OCB-B	w.r.	243	206	3.42	0.74498
OCB-C	w.r.	243	206	3.42	0.74434
OCB-D	w.r.	242	204	3.44	{ 0.74507 0.74502 *
OCB-E	w.r.	242	204	3.44	0.74515

w.r.= whole rock

* duplicate analysis

On a $^{87}\text{Sr}/^{86}\text{Sr}$ vs $^{87}\text{Rb}/^{86}\text{Sr}$ plot (Fig. 2), the biotite ratios do not form a linear array and appear to behave as open systems. Further, two aliquots of OCB-D biotite yielded different Rb and Sr abundances which were attributed to sample inhomogeneity. In Figure 2, two lines incorporate the data from each of the biotites with their corresponding whole-rock and feldspar data. Using the OCB-D biotite with the highest present-day $^{87}\text{Sr}/^{86}\text{Sr}$ ratio and the corresponding whole-rock and feldspar data, a date of ~360 Ma is obtained. Using the OCB-A data, a date of ~275 Ma is obtained, but this is associated with a high mean square of weighted deviates (MSWD) of 15, similar to that for the OCB-D line. An MSWD greater than ~3 for the present work indicates that the points do not approximate a straight line within experimental uncertainty.

Using only the whole rock and feldspar values gives a date of 305 ± 15 Ma, MSWD = 9 (Fig. 2 inset). An unusually high initial $^{87}\text{Sr}/^{86}\text{Sr}$ ratio ~0.727 (Table 2) suggests that the granite is derived from significantly older crust, or that an older system was reset at ~300 Ma. Based on the age discordances within Sedgwick pluton from previous K-Ar work, the mineral phases behaved as open systems and indicate post-intrusion disturbances in the isotopic systems. The data from the biotite sample OCB-D suggest that this intrusion could be older than 365 Ma.

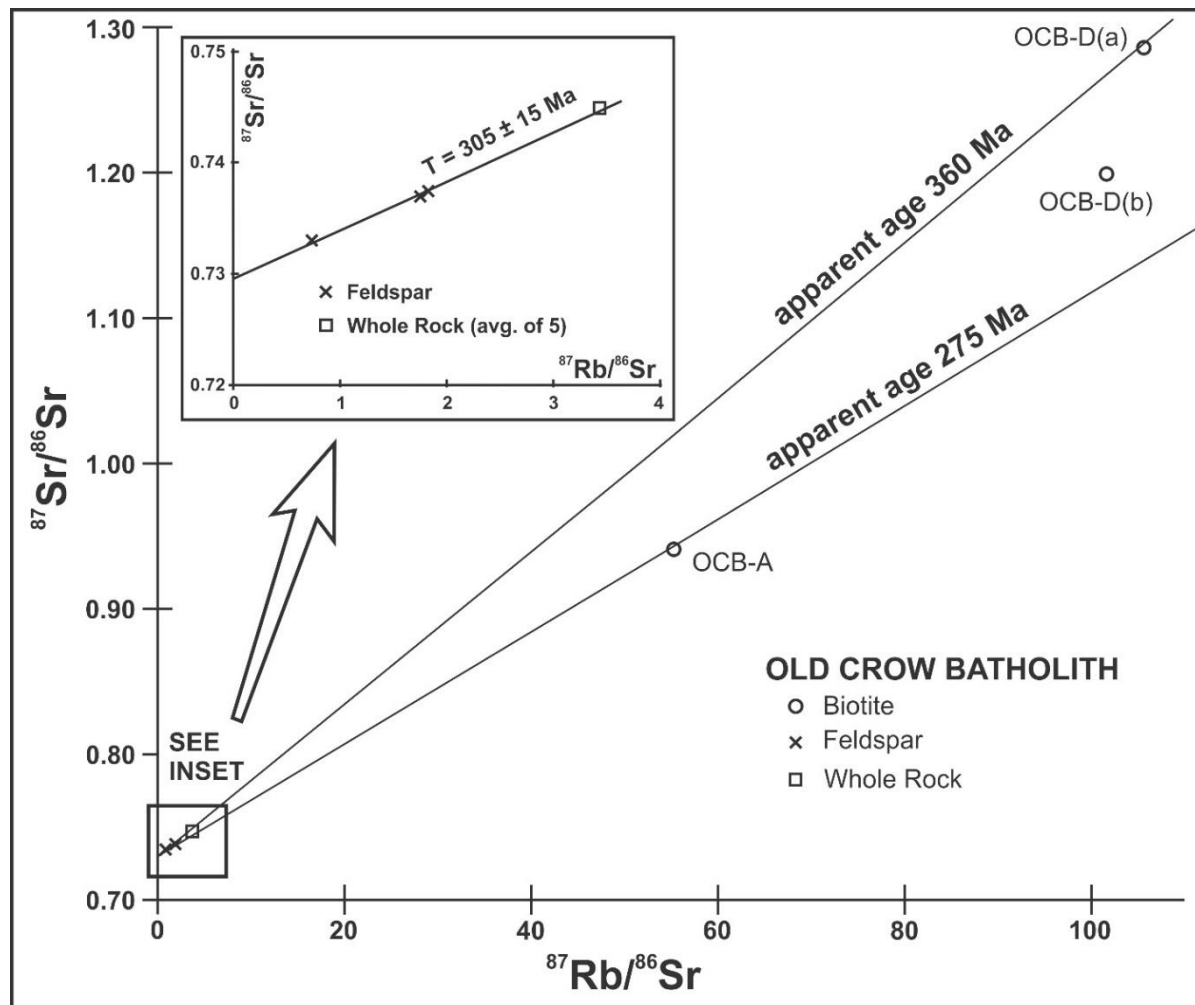


Figure 2. Rb-Sr whole rock and mineral isotopic ratios summarized from Figures 2 and 3 of Bell and Blenkinsop (1984).

**Appendix A: Part 2: Summary of
“Yukon Geochronological Project, 1984-1985 Final Report”**
K. Bell and J. Blenkinsop
(Figures and Tables numbered as in original report.)

Introduction-Methods-Results:

The aims of the project were: to define the ages of granitoid plutons in northern Yukon; and to assess from their $^{87}\text{Sr}/^{86}\text{Sr}$ initial ratios whether any of these plutons had been generated from continental crust. During the 1984 field season 48 samples were collected from six plutons: Ammerman, Dave Lord, Mt. Fitton, Mt Schaeffer, and Old Crow. Thin section and hand specimen examination showed that the Old Crow, Dave Lord and Mt. Sedgwick bodies were the least affected by weathering and/or alteration. Thus, further analyses were focused on these three plutons.

Representative samples from each of these bodies were slabbed and stained for potassium feldspar and plagioclase. The Dave Lord pluton was found to be an alkali feldspar syenite. Old Crow and Mt. Sedgwick plutons contain significant quartz and plagioclase. The former shows considerable variability but plots broadly within the granite field whereas the latter lies on the granite-monzonite boundary. The results are summarized on a Streckeisen diagram (Fig. 1).

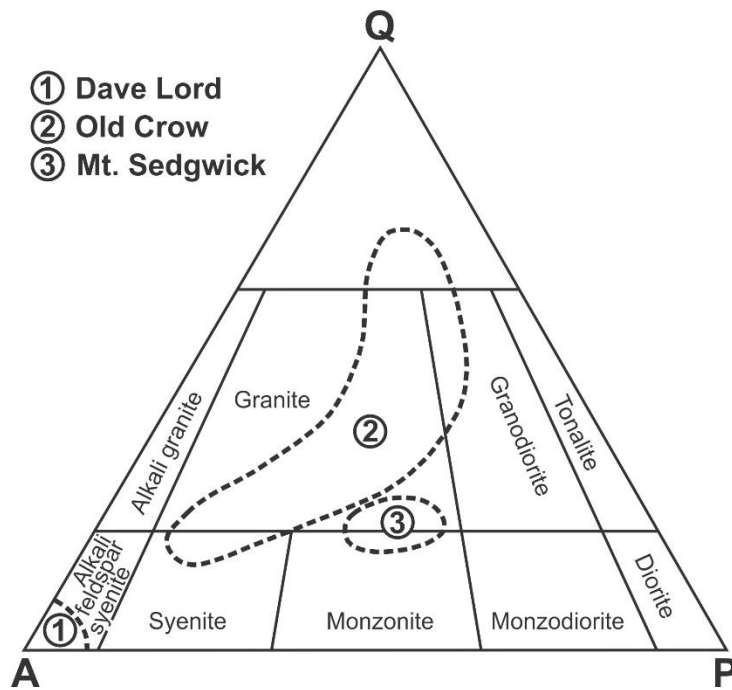


Figure 1. Streckeisen diagram. Rock names based on relative abundances of quartz (Q), alkali feldspar (A), and plagioclase (P).

Twenty-one samples were crushed to <100 mesh using a Bleuler mill. Rb and Sr abundances were determined by X-ray fluorescence, using the method of Norrish and Chappell (1967), in which the mass absorption coefficients are measured directly. Results are plotted in Table 1.

TABLE 1: Rb and Sr abundances and weight ratios:

<u>Sample No.</u>	<u>Rb (ppm)</u>	<u>Sr (ppm)</u>	<u>Rb/Sr (weight)</u>
<u>Dave Lord Pluton</u>			
DL 100	268	1540	0.174
DL 101	363	708	0.513
DL 102	277	1620	0.171
DL 103	392	739	0.530
DL 104	330	1150	0.287
DL 105	388	294	1.32
DL 106	355	698	0.509
DL 107	289	859	0.336
DL 108	378	320	1.18
<u>Old Crow Batholith</u>			
OCB 102	250	183	1.37
OCB 106	292	72.4	4.03
OCB 108	274	89.9	3.05
OCB 111	202	194	1.04
OCB 112	219	186	1.18
<u>Mt. Sedgwick</u>			
SE 100	195	695	0.281
SE 101	193	777	0.248
SE 102	194	647	0.300
SE 103	184	679	0.271
SE 104	199	628	0.317
SE 105	200	725	0.276
SE 106	188	666	0.282

Mt. Sedgwick has the lowest and most uniform Rb/Sr ratios, whereas Old Crow has the highest. The variation in Rb/Sr ratios is primarily due to variation in the Sr content. The Rb abundances are fairly constant, averaging 338 ppm in Dave Lord pluton, 193 ppm in Mt. Sedgwick and 247 ppm in Old Crow.

Five samples from each of the three plutons were chosen, based on their Rb/Sr ratios, for Sr isotopic analysis. Samples were dissolved in HF and HClO₄ and Sr was separated using ion-exchange chromatography. The Sr isotopic compositions were measured on a Finnigan-MAT 261 solid-source mass spectrometer in the static multicollector mode. Results are in Table 2.

TABLE 2 Isotopic Data:

<u>Sample No.</u>	<u>Rb (ppm)</u>	<u>Sr (ppm)</u>	<u>$^{87}\text{Sr}/^{86}\text{Sr}$ (atomic)</u>	<u>$^{87}\text{Rb}/^{86}\text{Sr}$ (atomic)</u>
<u>Dave Lord Pluton</u>				
DL 100	268	1540	0.70875	0.506
DL 101	363	708	0.71366	1.48
DL 105	388	294	0.72538	3.82
DL 107	289	859	0.71171	0.972
DL 108	378	320	0.72337	3.43
<u>Old Crow Batholith</u>				
OCB 102	250	183	0.74682	3.95
OCB 106	292	72.4	0.79105	11.8
OCB 108	274	89.9	0.77208	8.88
OCB 111	202	194	0.74438	3.02
OCB 112	219	186	0.74481	3.43
<u>Mt. Sedgwick</u>				
SE 100	195	695	0.71491	0.812
SE 101	193	777	0.71461	0.718
SE 102	194	647	0.71496	0.868
SE 104	199	628	0.71532	0.918
SE 105	200	725	0.71538	0.797

Notes:Reproducibility of Sr isotope ratio measurements is thought to be 0.00005 (2σ)All values normalized to a $^{86}\text{Sr}/^{88}\text{Sr}$ ratio of 0.1194

Value for the Eimer and Amend Sr standard was 0.70801

 ^{87}Rb decay constant used: $1.42 \times 10^{-11} \text{ yr}^{-1}$ Discussion of Results:

For Dave Lord pluton, four of five points define a straight line corresponding to a date of 352 ± 5 Ma and an initial $^{87}\text{Sr}/^{86}\text{Sr}$ ratio of 0.7062 ± 0.0001 (2σ in all cases) (Fig. 2). The mean square of weighted deviates (MSWD) is 0.1 for the four-point isochron. A value less than 2 is considered a good fit of the data points to a straight line.

New data from Old Crow batholith did not define an isochron, similar to the result from the preliminary study which was hampered by the limited spread of Rb/Sr ratios in the earlier data (Fig. 3). The new whole-rock data yields a least-squares fit corresponding to a date of 365 ± 8 Ma and an initial $^{87}\text{Sr}/^{86}\text{Sr}$ ratio of 0.7275 ± 0.0005 (Fig. 3). However, the scatter of the data

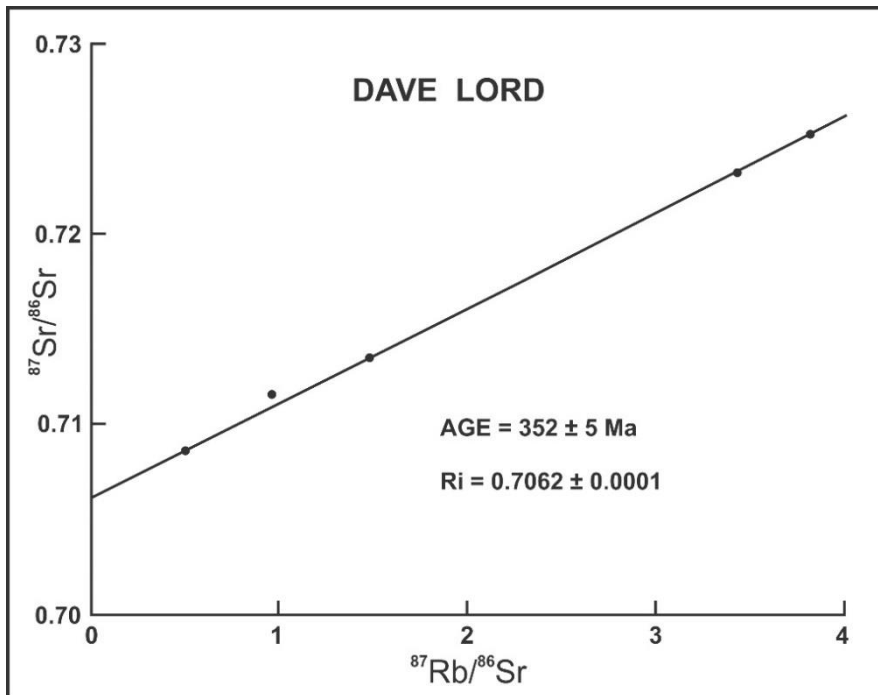


Figure 2. Rb-Sr isochron plot for Dave lord pluton.

(MSWD = 41) is so great that this line cannot represent an isochron. The scatter in the data reflects either post-crystallization isotopic disturbances, or alternatively, at the time of crystallization, the pluton did not have a uniform initial Sr isotopic composition. The latter could result from magma contamination, or by partial melting of continental crust which failed to mix completely prior to crystallization. The distribution of new data points above the 305 Ma regression (Fig. 3, Line A) suggests that the pluton is significantly older than 305 Ma.

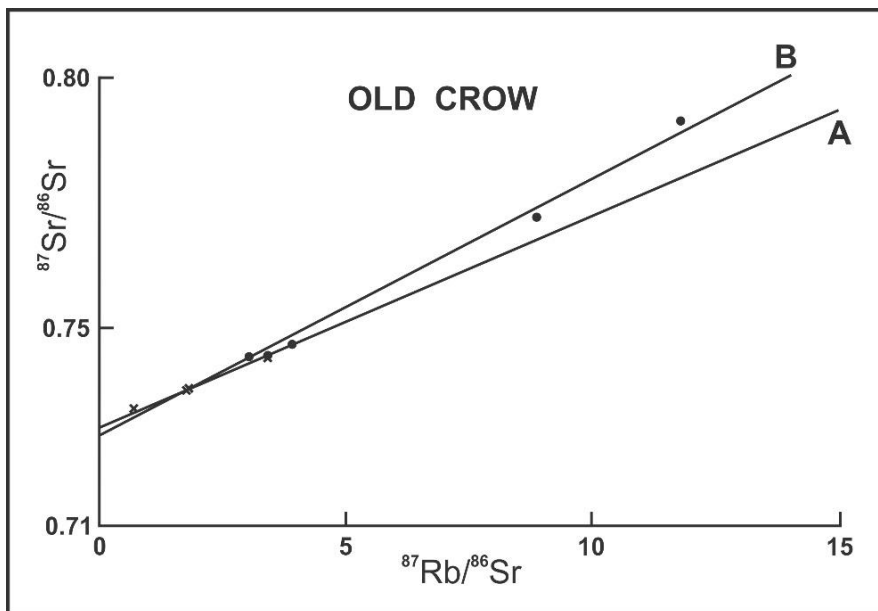


Figure 3. Rb-Sr plot for Old Crow batholith. Data from the preliminary study (Line A) produced a 305 ± 15 Ma age based on whole rock and feldspar data, whereas coexisting biotite did not fall on this line. A least-squares fit to the current data (Line B) indicates an age of 365 ± 8 Ma with MSWD = 41, too great to define an isochron.

For the Mt. Sedgwick pluton, a regression line is poorly resolved (Fig. 4) due to the restricted spread in Rb/Sr weight ratios (0.248 - 0.317). Using three of the five points a line can be fitted corresponding to a date of 249 ± 31 Ma (MSWD = 0.8). Whether this represents a geologically meaningful age is questionable.

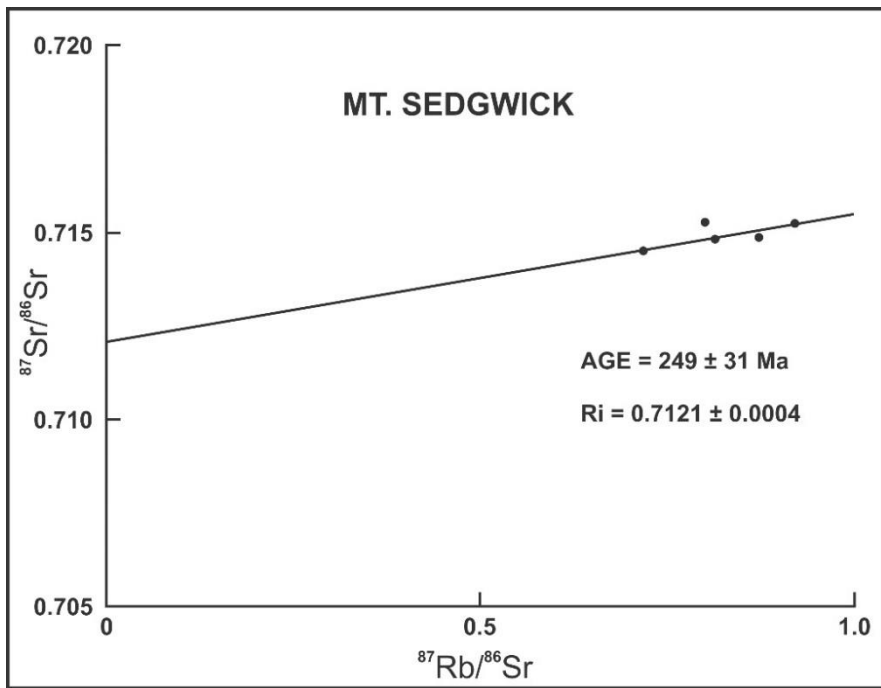


Figure 4. Rb-Sr data and 3-point regression line plot for Mt. Sedgwick pluton.

The scatter of the isotopic data from Old Crow and Mt. Sedgwick plutons is difficult to ascribe to a single cause. The petrographic evidence indicates a complex history involving alteration and/or metamorphism. Sericitization of feldspars and chloritization of biotite and amphibole is present in all three plutons. Two generations of mica occur in Old Crow and Mt. Sedgwick plutons. In thin section, hematite rims occur on feldspars from Dave Lord pluton. Despite the scatter in isotopic data from Old Crow and Mt. Sedgwick, we may calculate a maximum provenance age. Assuming closed system behaviour and an initial $^{87}\text{Sr}/^{86}\text{Sr}$ ratio of 0.702 (a realistic lower limit), the oldest permissible model age is about 1200 Ma for either pluton.

Conclusions:

1. A good isochron from Dave Lord pluton gives an age of 352 ± 5 Ma, with an initial $^{87}\text{Sr}/^{86}\text{Sr}$ ratio of 0.7062 ± 0.0001 , suggesting a low Rb/Sr source such as the lower crust or upper mantle.
2. The isotopic systems in Old Crow and Mt. Sedgwick plutons have been disturbed, or their initial Sr isotopic compositions were not uniform.
3. If the analytical data from Old Crow and Mt. Sedgwick plutons reflect their source ages, then that would be no more than ~ 1200 Ma.
4. The isotopic evidence from Old Crow and Mt. Sedgwick suggest a more complex geological history than that experienced by Dave Lord pluton.

APPENDIX B: DATA TABLES

Table B1: Sample Location Data

Geochemistry Sample Locations

C-Number	Sample Name	Prov/State	Location Type	Map Datum	North Latitude	West Longitude	Intrusion
C-154740	88LHA1-04B	Yukon	Outcrop	NAD83	68.4602985	138.0525486	Mt Fitton
C-154818	88LHA07-02	Yukon	Talus	NAD83	67.7575765	139.769393	Schaeffer
C-154819	88LHA07-04A	Yukon	Outcrop	NAD83	67.5672599	140.738299	Old Crow SE
C-154823	88LHA07-06	Yukon	Felsenmeer	NAD83	67.5941824	139.2395292	Dave Lord
C-194579	91ADO-201	Alaska	Outcrop	NAD83	67.741687	141.7194171	Old Crow NW
C-194580	91ADO-279	Yukon	Outcrop	NAD83	68.3897	142.1422	Bear Mtn porphyry
C-194581	91ADO-284A	Yukon	Outcrop	NAD83	68.4189565	141.8808497	Bear Mtn syenite
C-247032	93LHA8-6	Yukon	Talus	NAD83	68.3685755	140.9820052	Ammerman granite
C-247047	93LHA9-5A	Yukon	Outcrop	NAD83	67.7923629	140.6248011	Old Crow NE
C-247056	93LHA10-5	Yukon	Rubble	NAD83	68.383476	140.982307	Ammerman porph.
C-247128	93LHA27-2B	Yukon	Talus	NAD83	68.9021973	139.012016	Sedgwick NE
C-627455*	525NC-1	Yukon	unspecified	NAD83	68.848508	139.065735	Sedgwick SE

* Location modified from Norris (1981a) and Wanless et al. (1974), using satellite imagery

Geochronology Sample Locations

C-Number	Sample Name	Prov/State	Location Type	Map Datum	North Latitude	West Longitude	Intrusion
C-154740	88LHA1-04B	Yukon	Outcrop	NAD83	68.4602985	138.0525486	Mt Fitton
C-154818	88LHA07-02	Yukon	Talus	NAD83	67.7575765	139.7693931	Schaeffer
C-154819*	88LHA07-04A	Yukon	Outcrop	NAD83	67.5672599	140.738299	Old Crow SE
C-154823	88LHA07-06	Yukon	Felsenmeer	NAD83	67.5941824	139.2395292	Dave Lord
C-154882	88LHA17-08	Yukon	Talus	NAD83	68.5445006	138.1459654	Hoidahl
C-194566	80ABe-23D(X+Z)	Alaska	Talus	NAD83	68.3764416	141.0296525	Ammerman granite
C-194567	80ABe-23E	Alaska	Talus	NAD83	68.376475	141.0296081	Ammerman porph.
C-194579	91-ADo-201	Alaska	Outcrop	NAD83	67.741687	141.7194171	Old Crow NW
C-194580	91-ADo-279	Alaska	Outcrop	NAD83	68.3897	142.1422	Bear Mtn porphyry
C-194581	91-ADo-284a	Alaska	Outcrop	NAD83	68.4189565	141.8808497	Bear Mtn syenite

*same locality as C-080698 (62TI-103): 265±12 Ma K-Ar age

Table B2a. Major element chemistry north Yukon plutons

Sample	Rock Unit	SiO ₂	Al ₂ O ₃	TiO ₂	Fe ₂ O _{3(T)}	FeO _(T)	MgO	CaO	Na ₂ O	K ₂ O	P ₂ O ₅	MnO	LOI	TOTAL	Nb	Zr	Y	Sr	U	Rb	Th	Pb	Ba	Ni	Cr	Ga
C-154818	Schaeffer ¹	73.92	13.17	0.22	1.51	1.36	0.22	0.90	2.51	5.54	0.07	0.03	0.68	98.85	34	86	34	121	5	318	42	b.d.	507	9	46	n.d.
C-154819	Old Crow ¹	66.92	14.40	0.56	4.29	3.86	1.64	2.16	2.00	5.01	0.13	0.08	1.08	98.39	16	151	39	177	7	205	20	14	702	119	36	n.d.
C-247047	Old Crow NE ¹	67.78	13.82	0.55	4.00	3.60	1.26	1.97	2.32	4.76	0.14	0.06	2.27	99.05	4	116	29	137	b.d.	220	28	16	n.d.	n.d.	n.d.	n.d.
C-194579	Old Crow ¹	71.29	14.03	0.41	3.11	2.80	0.57	2.03	2.42	4.66	0.10	0.04	0.83	99.60	15	148	33	110	b.d.	166	22	17	490	52	38	n.d.
Bur-8	Old Crow ²	74.87	13.03	0.12	1.10	0.99	0.21	0.70	2.79	5.69	0.05	0.03	1.09	99.68	31	63	40	146	9.9	370	39	n.d.	220	n.d.	n.d.	23
C-154740	Fitton ¹	67.72	15.32	0.33	3.00	2.70	1.00	2.59	2.51	5.16	0.13	0.04	0.82	98.84	20	130	24	381	6	159	31	b.d.	1344	1	40	n.d.
525NC	Fitton ¹	75.64	12.81	0.19	1.13	1.02	0.23	0.94	2.61	5.28	0.02	0.01	1.04	99.99	24	68	17	89	17	232	32	8	372	0	52	n.d.
Bur-3	Fitton ²	65.15	15.27	0.49	5.28	4.75	2.61	2.92	2.18	4.66	0.14	0.07	1.57	100.33	17	151	23	319	3.07	208	16	n.d.	974	n.d.	n.d.	14
Bur-4	Fitton ²	69.66	13.88	0.34	3.75	3.38	1.20	2.82	3.13	3.80	0.22	0.05	0.69	99.53	22	191	20	398	9.41	197	45	n.d.	861	n.d.	n.d.	13
C-247128	Mt. Sedgwick ¹	67.00	15.54	0.43	3.68	3.31	1.08	2.15	2.57	4.66	0.22	0.03	2.42	99.97	14	124	20	287	b.d.	174	19	b.d.	n.d.	n.d.	n.d.	n.d.
Bur-1	Mt. Sedgwick ²	65.74	15.23	0.52	4.64	4.18	1.85	3.45	3.16	4.26	0.25	0.06	1.49	100.64	27	174	20	670	8.48	223	37	n.d.	854	n.d.	n.d.	18
Bur-2	Mt. Sedgwick ²	71.12	14.26	0.27	2.19	1.97	0.62	2.26	3.20	4.82	0.10	0.04	1.09	99.97	22	127	15	403	9.19	205	30	n.d.	1328	n.d.	n.d.	12
Bur-5	Hoidahl ²	64.65	15.05	0.42	5.73	5.16	2.42	3.42	2.78	3.56	0.12	0.11	2.36	100.59	17	146	18	309	4.15	166	14	n.d.	1014	n.d.	n.d.	15
Bur-6	Hoidahl ²	68.83	14.87	0.35	3.96	3.56	1.29	2.33	2.82	3.66	0.15	0.05	1.29	99.60	14	156	21	293	5.93	150	15	n.d.	1127	n.d.	n.d.	14
C-247032	Ammerman pluton ¹	73.09	13.83	0.21	2.27	2.04	0.37	2.06	2.61	3.81	0.04	0.07	1.08	99.52	b.d.	67	15	106	b.d.	190	22	14	n.d.	n.d.	n.d.	n.d.
Bur-7	Ammerman pluton ²	65.62	16.01	0.36	3.41	3.07	0.93	2.26	2.51	6.64	0.12	0.06	1.69	99.61	12	162	20	201	4.08	306	25	n.d.	967	n.d.	n.d.	15
C-247056	Ammerman porphyry ¹	75.32	12.82	0.22	0.83	0.75	0.15	0.16	2.42	4.89	0.03	<0.01	1.14	98.11	5	121	8	69	b.d.	169	24	16	n.d.	n.d.	n.d.	n.d.
C-154823	Dave Lord ¹	61.27	19.37	0.39	2.94	2.65	0.36	1.97	4.11	8.18	0.06	0.08	0.66	99.77	113	350	40	1211	b.d.	170	38	15	1505	14	20	n.d.
Bur-9	Dave Lord ²	55.35	22.34	0.23	2.90	2.61	0.05	2.17	1.81	11.25	0.04	0.18	3.15	99.47	536	756	16	1115	93.9	533	65	n.d.	907	n.d.	n.d.	26
Bur-10	Dave Lord ²	57.44	23.64	0.14	2.18	1.96	0.12	0.40	1.95	11.77	0.03	0.13	1.98	99.79	470	341	7	1215	83.7	603	44	n.d.	873	n.d.	n.d.	28
Bur-11	Dave Lord ²	59.82	20.38	0.35	3.20	2.88	0.50	0.45	3.63	9.93	0.09	0.17	1.76	100.26	164	354	28	1830	7.37	384	89	n.d.	1828	n.d.	n.d.	17
Bur-12	Dave Lord ²	62.79	18.01	0.14	2.00	1.80	0.07	2.91	5.82	7.74	0.01	0.11	0.70	100.29	228	965	36	647	22.7	317	77	n.d.	857	n.d.	n.d.	31
Bur-13	Dave Lord ²	52.26	20.95	0.30	4.32	3.89	0.16	4.79	4.50	8.01	0.03	0.25	4.07	99.64	531	1076	18	2605	96.2	381	72	n.d.	741	n.d.	n.d.	27
Bur-14	Dave Lord ²	54.16	21.64	0.16	2.70	2.43	0.07	2.16	8.56	8.58	0.03	0.17	1.08	99.31	287	1123	5	958	41.3	438	40	n.d.	531	n.d.	n.d.	33
C-194580	Bear Mt. porphyry ¹	77.81	13.47	0.38	0.76	0.68	0.52	0.03	0.21	3.98	0.10	0.02	2.16	99.46	33	169	18	5	b.d.	200	14	b.d.	167	3	27	n.d.
C-194581	Bear Mt. pluton ¹	62.21	16.49	0.76	4.59	4.13	1.04	2.16	4.01	6.20	0.23	0.15	1.86	99.81	133	695	70	256	9	277	78	32	634	21	23	n.d.

Data Sources: 1 this study; 2 Burwash, 1997.

Total Fe reported as Fe₂O_{3(T)}. FeO_(T) calculated from measured Fe₂O_{3(T)}.

Minor and trace element values expressed as parts per million (ppm). b.d. - below detection limit; n.d. - not determined.

For samples in our study, major elements determined by XRF (ME-XRF06 analytical package) from ALS Chemex Laboratories, N. Vancouver, Canada; minor and trace element analyses performed at GSC Calgary.

Table B2b. Major element chemistry north Yukon plutons (GSC Calgary analyses 1993-94)

curation #	field #	Pluton	FE2O3	MNO	CR2O3	TIO2	BAO	CAO	K2O	P2O5	SIO2	AL2O3	MGO	NA2O	LOI	TOTAL
Lab Report date: 1993-05-06																
C-154740	88LHA1-4B	Mt Fitton	3.01	0.05		0.31	0.15	2.68	5.39	0.14	68.82	15.33	1.06	2.15	0.90	99.99
C-154818	88LHA7-2	Schaeffer	1.49	0.04		0.20	0.05	0.78	5.69	0.05	75.43	13.44	0.27	1.96	0.60	100.00
C-154819	88LHA7-4A	Old Crow SE	4.45	0.08		0.52	0.07	1.99	5.13	0.12	68.47	14.80	1.73	1.62	1.00	99.98
C-154823	88LHA7-6	Dave Lord	2.84	0.10		0.42	0.15	1.76	8.23	0.06	61.98	18.23	0.37	5.14	0.70	99.98
C-627455	525NC-1	Sedgwick	1.22	0.02		0.15	0.05	0.90	5.55	0.03	76.32	12.74	0.23	1.69	1.10	100.00
C-194579	91ADO-201	Old Crow NW	3.45	0.05		0.37	0.06	1.84	4.87	0.07	72.06	14.16	0.57	1.70	0.80	100.00
C-194580	91ADO-279	Bear Mt. porphyry	0.89	0.02		0.36	0.02	0.04	4.29	0.10	78.02	13.53	0.54	0.09	2.10	100.00
C-194581	91ADO-284	Bear Mt. granite	5.46	0.18		0.78	0.09	2.17	6.89	0.26	61.72	15.75	1.03	4.07	1.60	100.00
Lab Report date: 1994-08-29																
C-247032	93LHA8-6	Ammerman granite	2.24	0.08	0.013	0.18	0.005	2.05	3.92	0.05	73.56	13.4	0.41	2.81	1.3	100.06
C-247056	93LHA10-5	Ammerman porphyry	0.83	0.02	0.01	0.19	0.13	0.2	5.14	0.03	76.67	12.79	0.16	2.69	1.25	100.09
C-247128	93LHA27-2B	Sedgwick NE	3.78	0.05	0.013	0.41	0.14	2.22	4.75	0.21	67.6	14.7	1.06	2.64	2.48	100.05
C-247047	93LHA9-5A	Old Crow NE	4.39	0.06	0.011	0.53	0.09	2.02	5.03	0.14	68.14	13.61	1.22	2.41	2.44	100.08

METHOD: Samples were mixed with a flux and fused at 1000°C to make a glass bead. All analyses were done on this bead. Analyses performed at GSC Calgary.

Note: Values expressed as % oxide.

Table B2c. Minor / Trace element chemistry north Yukon plutons (GSC Calgary analyses 1993-94)

curation #	field #	Pluton	MO	NB	ZR	Y	SR	U	RB	TH	PB	BA	ZN	CU	NI	MN	CR
Lab Report date: 1993-05-06																	
C-154740	88LHA1-4B	Mt. Fitton	bd	20	130	24	381	6	159	31	bd	1344	1	0	1	439	40
C-154818	88LHA7-2	Schaeffer	bd	34	86	34	121	5	318	42	bd	507	0	0	9	350	46
C-154819	88LHA7-4A	Old Crow SE	bd	16	151	39	177	7	205	20	14	702	26	0	119	655	36
C-154823	88LHA7-6	Dave Lord	bd	113	350	40	1211	bd	170	38	15	1505	17	0	14	796	20
C-627455	525NC-1	Sedgwick	bd	24	68	17	89	17	232	32	8	372	0	0	0	165	52
C-194579	91ADO-201	Old Crow NW	bd	15	148	33	110	bd	166	22	17	490	21	0	52	421	38
C-194580	91ADO-279	Bear Mt. porphyry	bd	33	169	18	5	bd	200	14	bd	167	0	0	3	192	27
C-194581	91ADO-284	Bear Mt. granite	3	133	695	70	256	9	277	78	32	634	58	0	21	1419	23
Lab Report date: 1994-08-29																	
C-247032	93LHA8-6	Ammerman granite	bd	bd	67	15	106	bd	190	22	14						
C-247056	93LHA10-5	Ammerman porphyry	bd	5	121	8	69	bd	169	24	16						
C-247047	93LHA9-5A	Old Crow NE	bd	4	116	29	137	bd	220	28	16						
C-247128	93LHA27-2B	Sedgwick NE	bd	14	124	20	287	bd	174	19	bd						
AVERAGE DETECTION LIMITS:																	
			4	3	5	5	5	10	15	12	14	28	5	5	5	6	6

Notes: bd - below detection limit. Values expressed as parts per million (ppm).

Table B3a. Rb-Sr and Sm-Nd isotopic data for northern Yukon intrusions

Intrusion	Sample	Source	Age	Rb (ppm)	Sr (ppm)	87Rb/ 86Sr	87Sr/ 86Sr	error (2σ)	Sr initial	Sm (ppm)	Nd (ppm)	147Sm/ 144Nd	143Nd/ 144Nd	error (2σ)	ϵ Nd(t)	TDM(Ga)
Schaeffer	88LHA-07-02	3	366.5	469.7	139.7	9.785	0.7642	0.00019	0.712788	7.51	42.41	0.1071	0.512009	0.000007	-8.1	1.64
Old Crow	88LHA-07-04A	3	367.5	264.9	219.3	3.509	0.743273	0.00021	0.724838	7.49	38.31	0.1184	0.511878	0.000006	-11.1	1.86
Dave Lord	88LHA-07-06	3	366.6	219.8	1540	0.4128	0.708797	0.00033	0.706628	18.05	130.2	0.0838	0.51216	0.000008	-4	1.17
Sedgwick	525-NC	3	370	n.d.	n.d.					2.78	20.72	0.0809	0.51199	0.000011	-7.2	1.39
Sedgwick	525-NC (dup)	3	370	n.d.	n.d.					2.84	21.21	0.0808	0.511991	0.000006	-7.3	1.34
Hoidahl	88LHA-17-08	3	366.7	170.7	295.9	1.671	0.723994	0.00031	0.715213	3.83	23.15	0.0999	0.511946	0.000005	-8.9	1.62
Fitton	88LHA-01-04B	3	368.1		1.388	0.72223			0.71494							
Old Crow	OCB-A	1	367.5	204	206	3.38	0.74408			0.72627						
Old Crow	OCB-A: fs-lt	1	367.5	263	420	1.82	0.73749									
Old Crow	OCB-A: fs-hvy	1	367.5	128	506	0.735	0.73306									
Old Crow	OCB-A: bi	1	367.5	542	28.9	55.3	0.94066									
Old Crow	OCB-B	1	367.5	243	206	3.42	0.74498			0.72696						
Old Crow	OCB-C	1	367.5	243	206	3.42	0.74434			0.72632						
Old Crow	OCB-D	1	367.5	242	204	3.44	0.74507			0.72695						
Old Crow	OCB-D: fs	1	367.5	237	394	1.74	0.73698									
Old Crow	OCB-D: bi(a)	1	367.5	593	17.1	106	1.2820									
Old Crow	OCB-D: bi(b)	1	367.5	748	22.1	102	1.1979									
Old Crow	OCB-E	1	367.5	242	204	3.44	0.74515			0.72703						
Old Crow	OCB-102	2	367.5	250	183	3.95	0.74682			0.72601						
Old Crow	OCB-106	2	367.5	292	72.4	11.8	0.79105			0.72889						
Old Crow	OCB-108	2	367.5	274	89.9	8.88	0.77208			0.7253						
Old Crow	OCB-111	2	367.5	202	194	3.02	0.74438			0.72847						
Old Crow	OCB-112	2	367.5	219	186	3.43	0.74481			0.72674						
Sedgwick	SE-100	2	370	195	695	0.812	0.71491			0.71063						
Sedgwick	SE-101	2	370	193	777	0.718	0.71461			0.71083						
Sedgwick	SE-102	2	370	194	647	0.868	0.71496			0.71039						
Sedgwick	SE-104	2	370	199	628	0.918	0.71532			0.71048						
Sedgwick	SE-105	2	370	200	725	0.797	0.71538			0.71118						
Dave Lord	DL-100	2	366.6	268	1540	0.506	0.70875			0.70614						
Dave Lord	DL-101	2	366.6	363	708	1.48	0.71366			0.70601						
Dave Lord	DL-105	2	366.6	388	294	3.82	0.72538			0.70564						
Dave Lord	DL-107	2	366.6	289	859	0.972	0.71171			0.70669						
Dave Lord	DL-108	2	366.6	378	320	3.43	0.72337			0.70565						

Table B3b. Sm-Nd isotopic data for northern Yukon metasedimentary rocks

Unit	Sample	Source	Age	Lithology	Sm (ppm)	Nd (ppm)	147Sm/ 144Nd	143Nd/ 144Nd	error (2σ)	ϵ Nd(t)	Map Datum	N. Lat.	W. Long.	
unnamed	250NC*	3	Proterozoic?	quartzite	1.42	6.42	0.1338	0.51211	0.000007	-7.3	1.78	NAD83	67.7830747	139.9359944
Whale Mtn	87LHA-7-1B	3	Cambrian	argillite	5.56	29.66	0.1133	0.511862	0.000008	-11.2	1.96	NAD83	69.1687194	140.8749679
"Neruokpuk"	524NC-1*	3	Prot-Camb	quartzite	9.71	47.14	0.1245	0.511593	0.000003	-17.1	2.49	NAD83	68.9080978	139.0027167
unnamed	90LHA-19-1A	3	Ediacaran?	limestone	0.55	3.01	0.1098	0.511671	0.000010	-14.8	2.17	NAD83	69.4012205	140.970166
"Neruokpuk"	90LHA-14-1B	3	Cambrian?	quartzite	5.21	27.81	0.1132	0.511417	0.000009	-19.9	2.62	NAD83	69.3034249	140.3559464
Red argillite	90LHA-7-1	3	Cambrian	argillite	7.87	48.61	0.0978	0.511407	0.000007	-19.4	2.29	NAD83	69.4631205	140.9607648
Red argillite	210NC*	3	Cambrian	argillite	6.66	39.08	0.1031	0.511479	0.000007	-18.2	2.3	NAD83	69.3331234	139.5527022

* locations are approximate (from archived data in curation database). Sources: 1 = Bell and Blenkinsop (1984); 2 = Bell and Blenkinsop (1985); 3 = this study

Table B4. U-Pb TIMS analyses of zircon and titanite

Sample Description ^a	Wt	U (ppm)	Pb (ppm) ^b	206Pb/204Pb (meas.) ^c	common Pb (total, pg)	%208Pb	207Pb/235U ^d	(± % 1σ)	206Pb/238U ^d	(± % 1σ)	Rho	207Pb/206Pb ^d	(± % 1σ)	206Pb/238U age (Ma)	(± 2σ)	207Pb/235U age (Ma)	(± 2σ)	207Pb/206Pb age (Ma)	(± 2σ)
Sample 1 (88-LHA-07-04-a - Old Crow Batholith)																			
A: N1,+105	0.01	377	24.3	119	100	12.5	0.4741	1.54	0.06197	0.44	0.7	0.05549	1.28	387.6	3.3	394	10.1	432.2	57.2
B: N1,+105	0.01	634	38.1	319	46	11.6	0.4371	0.73	0.05864	0.19	0.6	0.05406	0.64	367.3	1.3	368.2	4.5	373.6	28.6
C: N1,+105	0.02	652	52.5	2279	28	10.4	0.9479	0.12	0.07702	0.09	0.9	0.08926	0.06	478.3	0.9	677	1.2	1409.8	2.3
D: N1,-105	0.01	208	12.1	228	21	9.7	0.4295	1.07	0.05763	0.21	0.6	0.05405	0.95	361.2	1.4	363.8	6.5	373.3	42.7
E: N1,+149	0.17	729	44.2	11540	39	9	0.5022	0.34	0.06051	0.33	1	0.06019	0.05	378.7	2.4	413.2	2.3	610.2	1.9
F: N1,+149	0.19	680	40.2	873	561	10	0.4386	0.27	0.05873	0.19	0.8	0.05416	0.16	367.9	1.3	369.3	1.7	377.8	7.1
G: N1,+105	0.02	608	34.2	4126	10	9.5	0.4160	0.2	0.05609	0.12	0.8	0.05379	0.12	351.8	0.9	353.2	1.2	362.2	5.4
H: N1,+105	0.01	667	39.2	11070	3	9.9	0.4340	0.2	0.05837	0.15	0.9	0.05393	0.11	365.7	1	366	1.3	368.1	4.8
I: N1,+105	0.02	533	31.9	8987	4	10.1	0.4502	0.18	0.05929	0.12	0.8	0.05507	0.11	371.3	0.9	377.4	1.2	415.2	4.7
Sample 2 (91-ADo-201 - Old Crow Batholith)																			
A: N2,+134	0.03	177	10.9	4579	5	13.9	0.4394	0.28	0.05901	0.14	0.5	0.05401	0.24	369.6	1	369.8	1.7	371.3	10.6
B: N2,+134	0.03	456	26.4	927	49	10.6	0.4244	0.31	0.05717	0.14	0.8	0.05384	0.22	358.4	0.9	359.2	1.9	364.4	10
C: N2,+134	0.02	315	18.6	3818	7	10.6	0.4333	0.25	0.05825	0.21	0.8	0.05395	0.15	365	1.5	365.5	1.6	369.1	6.9
D: N2,+134	0.04	346	22.2	12740	4	11.9	0.4865	0.26	0.06216	0.22	0.9	0.05676	0.09	388.7	1.6	402.5	1.7	482.1	3.9
E: N2,+134	0.05	259	15.7	11630	4	17	0.4401	0.2	0.05879	0.13	0.8	0.0543	0.12	368.2	1	370.3	1.2	383.5	5.5
Sample 3 (88-LHA-07-02 - Schaeffer pluton)																			
A: N1,+105	0.02	600	33.4	921	35	14.4	0.3899	0.26	0.05253	0.1	0.6	0.05383	0.22	330	0.6	334.3	1.5	364.1	9.9
B: N1,+105	0.01	465	28.9	683	25	16.4	0.4254	0.45	0.05735	0.12	0.6	0.0538	0.4	359.5	0.8	359.9	2.7	362.6	17.9
C: N1,+105	0.01	197	14.2	291	32	25.8	0.4397	0.57	0.059	0.18	0.7	0.05405	0.48	369.6	1.3	370	3.5	373	21.5
D: N1,-105	0.02	374	25.6	813	34	22.8	0.4332	0.4	0.05816	0.11	0.6	0.05403	0.35	364.4	0.8	365.5	2.5	372.2	15.9
E: N2,+105	0.08	332	20.8	4382	21	18.3	0.4200	0.42	0.05636	0.33	0.9	0.05404	0.17	353.5	2.2	356	2.5	372.9	7.5
F: N2,+105	0.06	295	17.4	1553	36	18.9	0.3953	0.47	0.05285	0.33	0.9	0.05425	0.23	332	2.1	338.2	2.7	381.5	10.4
H: N2,+105	0.03	327	20.5	2548	11	19.9	0.4096	0.22	0.05521	0.13	0.9	0.0538	0.13	346.4	0.9	348.6	1.3	362.8	5.7
I: N2,+105	0.02	358	22.5	3100	8	18.8	0.4185	0.22	0.05637	0.15	0.8	0.05386	0.13	353.5	1	355	1.3	365	5.9
Sample 4 (88-LHA-17-08 - Hoidahl Cupola)																			
A: N1,+105	0.06	906	51.4	899	214	7.3	0.4331	0.33	0.05803	0.11	0.6	0.05413	0.29	363.6	0.8	365.4	2.1	376.4	12.8
B: N1,+105	0.02	946	53.7	2219	26	7.4	0.4326	0.16	0.05799	0.09	0.7	0.05411	0.12	363.4	0.6	365	1	375.5	5.5
C: N1,-105	0.01	861	49.6	859	29	9.2	0.4306	0.36	0.05772	0.12	0.6	0.05411	0.31	361.7	0.8	363.6	2.2	375.8	13.9
D: N2,+149	0.13	828	44	3175	110	7.9	0.4029	0.35	0.054	0.33	1	0.0541	0.07	339.1	2.2	343.7	2	375.4	3
E: N2,105-149	0.16	913	50	1830	270	7.7	0.4163	0.36	0.0558	0.33	1	0.05411	0.09	350	2.3	353.4	2.1	375.6	4.1

Sample 5 (88-LHA-01-04b - Mt. Fitton pluton)																			
A: N1,+149	0.04	1119	62.5	7576	19	13.2	0.3989	0.11	0.05347	0.09	0.9	0.05411	0.04	335.8	0.6	340.8	0.6	375.5	2
B: N1,105-149	0.04	1007	58.3	5613	22	13.3	0.4127	0.13	0.05535	0.11	0.9	0.05407	0.06	347.3	0.8	350.8	0.8	374	2.8
C: N1,105-150	0.02	926	58.5	315	243	13.7	0.4698	0.56	0.0599	0.17	0.7	0.05688	0.46	375	1.3	391.1	3.6	487	20.3
D: N1,105-149	0.08	463	27	7293	18	12.8	0.4160	0.32	0.05596	0.31	1	0.05391	0.06	351	2.1	353.2	1.9	367.2	2.8
E: N1,105-150	0.03	536	32.1	2546	23	13.4	0.4295	0.4	0.05765	0.14	0.6	0.05404	0.34	361.3	1	362.8	2.4	372.8	15.5
Sample 6 (C-194566 - Ammerman granodiorite)																			
A: N2,+149	0.11	176	12.6	15360	4	24.9	0.4420	0.19	0.05924	0.12	0.9	0.05412	0.11	371	0.9	371.7	1.2	376	4.8
C: N2,+149	0.1	172	12.3	9346	7	24.4	0.4443	0.2	0.05952	0.1	0.8	0.05415	0.14	372.7	0.7	373.3	1.2	377.2	6.2
D: N2,+149	0.09	129	9	10390	4	22.4	0.4433	0.2	0.05949	0.13	0.9	0.05405	0.1	372.5	1	372.6	1.2	373	4.5
Sample 8 (88-LHA-07-06 - Dave Lord Pluton)																			
A: N1,+105	0.04	489	32.8	206	451	21	0.4448	0.84	0.05836	0.41	0.5	0.05529	0.72	365.6	2.9	373.7	5.3	423.8	32.3
E: N1,+149	0.15	424	27.7	9058	24	17.3	0.4333	0.48	0.05794	0.42	1	0.05424	0.14	363.1	2.9	365.5	2.9	380.8	6.4
G: N1,+149	0.15	161	10.7	7008	12	20.9	0.4342	0.4	0.05812	0.32	0.9	0.05418	0.15	364.2	2.3	366.2	2.5	378.5	6.7
H: N1,+149	0.19	353	23.4	13610	17	21	0.4293	0.32	0.05771	0.31	1	0.05395	0.05	361.7	2.2	362.7	1.9	368.8	2.3
I: N1,+149	0.15	334	22.6	8313	6	22.1	0.4287	0.29	0.05791	0.24	0.9	0.05369	0.15	362.9	1.7	362.2	1.8	357.9	6.5
J: N1,+149	0.05	366	23.4	9028	7	19.3	0.4230	0.2	0.05703	0.14	0.9	0.05379	0.09	357.6	1	358.2	1.2	362.2	4.2
K: N1,+149	0.05	334	22.5	11640	5	22.1	0.4298	0.2	0.05778	0.12	0.8	0.05395	0.12	362.1	0.9	363	1.2	369	5.2
T1: titanite,u	0.14	167	16.3	328	270	46.1	0.4298	0.71	0.05781	0.18	0.7	0.05393	0.6	362.3	1.3	363	4.4	367.9	27.1
T2: titanite,u	0.16	172	17.2	255	409	47.8	0.4266	0.81	0.05715	0.23	0.7	0.05414	0.66	358.3	1.6	360.7	4.9	376.7	29.6
Sample 9 (91-Ado-284a - Bear Mountain pluton)																			
A: N2,+134	0.18	569	5.2	1296	41	18.2	0.0534	0.54	0.00823	0.2	0.5	0.047064	0.48	52.8	0.2	52.8	0.6	52.5	22.7
B: N2,+134	0.22	705	6.2	1621	47	17.1	0.0529	0.64	0.00813	0.16	0.4	0.04721	0.6	52.2	0.2	52.4	0.7	59.6	28.5
C: N2,+134	0.22	618	5.5	1599	43	18	0.0529	0.31	0.00815	0.16	0.7	0.04707	0.22	52.4	0.2	52.4	0.3	53	10.3
D: N2,+134	0.16	788	7	370	183	16.9	0.0531	1.07	0.00817	0.13	0.5	0.04709	1.013	52.5	0.1	52.5	1.1	53.9	48.1
Sample 10 (91-Ado-279 - Bear Mountain rhyolite porphyry dyke)																			
A: N2,+149	0.05	1256	11.5	250	133	15.9	0.0559	0.83	0.00855	0.26	0.7	0.04745	0.68	54.9	0.3	55.3	0.9	71.8	32.1
B: N2,+149	0.04	513	4.5	3071	4	14.8	0.0543	0.68	0.00837	0.56	0.8	0.04709	0.4	53.7	0.6	53.7	0.7	53.6	18.8
C: N2,+149	0.07	728	6.4	1463	18	14.8	0.0549	0.43	0.00837	0.25	0.7	0.0476	0.33	53.7	0.3	54.3	0.5	79.4	15.6
D: N2,+149	0.06	922	8.3	1604	29	15.2	0.0554	0.26	0.00845	0.13	0.8	0.04755	0.18	54.3	0.1	54.8	0.3	77	8.7

^a N1, 2 = non-magnetic at 1 OR 2 degrees side slope on Frantz magnetic separator; grain size given in microns; u = abraded; ^b radiogenic Pb; corrected for blank, initial common Pb, and spike; c corrected for spike and fractionation as determined from replicate analyses of NBS common Pb standards; ^d corrected for 5-16 pg blank Pb and 1-2 pg blank U, and initial common Pb (from Stacey and Kramers, 1975). Errors associated with calculated ages were determined using the numerical error propagation method of Roddick (1987) and are given at the 2s level.

Table B5. Laser ablation ICP-MS analyses of zircon from Paleozoic and Tertiary intrusions in northern Yukon and northeastern Alaska

Analysis	Isotopic ratios						Isotopic ages						Background subtracted mean counts per second									
	207Pb/206Pb	1 σ	207Pb/235U	1 σ	206Pb/238U	1 σ	Rho	207Pb/206Pb	1 σ	207Pb/235U	1 σ	206Pb/238U	1 σ	202	204	206	207	208	232	235	238	Th/U
Sample 1 (88LHA-07-04A - Old Crow batholith)																						
1	0.05411	0.00065	0.43699	0.00578	0.05827	0.00029	0.38	375.5	26.83	368.1	4.09	365.1	1.76	22	0	26621	1453	2791	63245	3242	490341	0.13
2	0.05513	0.00073	0.4388	0.00641	0.05881	0.00032	0.37	417.2	28.95	369.4	4.53	368.4	1.95	21	17	32586	1811	3770	86423	4028	594811	0.15
3	0.0544	0.00093	0.44119	0.00836	0.05996	0.00041	0.36	387.8	37.62	371.1	5.89	375.4	2.5	43	7	28213	1547	3810	91876	3424	505219	0.18
4	0.05356	0.00073	0.41948	0.00631	0.05684	0.00032	0.37	352.5	30.45	355.7	4.52	356.4	1.93	54	12	18616	1005	2472	59477	2340	351788	0.17
5	0.05629	0.00144	0.45659	0.01309	0.05826	0.00059	0.35	463	56.4	381.9	9.13	365	3.62	58	16	14927	847	1450	33127	1812	275282	0.12
6	0.05372	0.00094	0.43538	0.00843	0.05883	0.00041	0.36	359.4	38.98	367	5.96	368.5	2.48	0	0	18666	1010	1978	48772	2269	341025	0.14
7	0.05387	0.00109	0.43078	0.00968	0.05892	0.00047	0.35	365.4	45.14	363.7	6.87	369	2.84	0	23	12673	687	1660	38468	1561	231250	0.17
8	0.05304	0.00192	0.4364	0.01759	0.05826	0.00081	0.34	330.6	80.04	367.7	12.44	365	4.93	0	0	12568	671	1907	46262	1506	231986	0.20
9	0.0538	0.00115	0.43095	0.01024	0.05834	0.00049	0.35	362.5	47.63	363.9	7.26	365.5	2.98	4	16	14285	773	1686	41073	1758	263374	0.16
10	0.05428	0.00112	0.42119	0.0096	0.05886	0.00048	0.36	382.5	45.56	356.9	6.86	368.7	2.9	14	0	13596	743	1348	31913	1728	248544	0.13
11	0.05282	0.00084	0.43345	0.00765	0.05839	0.00037	0.36	320.8	35.71	365.6	5.42	365.8	2.23	0	0	13232	703	1491	36244	1591	243930	0.15
12	0.05362	0.00077	0.44605	0.00716	0.06045	0.00035	0.36	355.2	32.36	374.5	5.03	378.3	2.13	46	22	17378	937	2006	47759	2062	309620	0.15
13	0.05379	0.00091	0.43573	0.00817	0.05897	0.0004	0.36	362.2	37.89	367.2	5.78	369.4	2.42	21	0	20713	1120	2432	52642	2525	378340	0.14
14	0.05354	0.00067	0.43177	0.006	0.05875	0.0003	0.37	351.5	27.99	364.4	4.25	368	1.85	24	17	30165	1624	3164	73213	3695	553277	0.13
15	0.0538	0.00106	0.43647	0.00956	0.05889	0.00046	0.36	362.5	43.92	367.8	6.76	368.8	2.8	0	17	24818	1342	3301	73560	3023	454339	0.16
16	0.05482	0.00086	0.44092	0.00768	0.05874	0.00037	0.36	404.9	34.48	370.9	5.41	367.9	2.25	38	3	14802	815	1462	30891	1819	271750	0.11
17	0.05408	0.00082	0.4324	0.00729	0.05856	0.00036	0.36	374.3	34.06	364.9	5.17	366.9	2.17	33	0	15071	819	3509	79558	1864	277587	0.29
18	0.05406	0.00069	0.43496	0.0062	0.0586	0.00031	0.37	373.3	28.84	366.7	4.39	367.1	1.89	38	0	24778	1345	2895	66942	3046	456154	0.15
19	0.05437	0.00069	0.4414	0.00626	0.05889	0.00031	0.37	386.1	28.39	371.2	4.41	368.9	1.89	46	0	38542	2104	3313	72535	4696	706274	0.10
Sample 2 (91ADo-201 - Old Crow batholith)																						
1	0.06042	0.00435	0.44168	0.03557	0.05814	0.00162	0.35	618.7	148.2	371.4	25.06	364.3	9.88	45	12	2069	124	288	7836	250	52540	0.15
2	0.0535	0.00158	0.46704	0.01568	0.06147	0.0007	0.34	350	65.46	389.1	10.85	384.5	4.28	4	0	13456	719	3596	103191	1365	323357	0.32
3	0.05419	0.00163	0.42881	0.01445	0.05762	0.00067	0.35	378.9	66.07	362.3	10.27	361.1	4.06	0	10	6408	347	1126	37217	717	164375	0.23
4	0.05277	0.002	0.43697	0.01861	0.05836	0.00083	0.33	318.7	83.8	368.1	13.15	365.6	5.05	0	0	4517	238	737	24486	483	114474	0.21
5	0.05237	0.00227	0.43545	0.02129	0.05806	0.00094	0.33	301.7	96.01	367	15.06	363.8	5.73	0	15	4484	234	615	16845	478	114279	0.15
6	0.05033	0.00227	0.42852	0.02175	0.05839	0.00097	0.33	210.3	101.3	362.1	15.46	365.9	5.89	0	0	4452	223	753	21062	465	112948	0.19
7	0.05431	0.00338	0.4428	0.03116	0.05824	0.00138	0.34	383.8	134	372.2	21.93	364.9	8.38	36	0	3111	168	585	20026	339	79173	0.25
8	0.05486	0.00169	0.43418	0.01496	0.05815	0.00069	0.34	406.3	66.73	366.1	10.59	364.4	4.18	6	0	4366	239	1053	32435	491	111342	0.29
9	0.05189	0.00272	0.42782	0.02523	0.05816	0.00113	0.33	280.4	115.9	361.6												

19	0.04914	0.00337	0.39307	0.02977	0.05703	0.00135	0.31	154.6	153.2	336.6	21.7	357.5	8.24	0	15	1782	87	302	9911	200	46705	0.21
20	0.05438	0.00342	0.43258	0.03041	0.05859	0.00135	0.33	386.6	135.2	365	21.55	367	8.2	0	0	1601	86	315	10423	181	40867	0.26
Sample 3 (88LHA-07-02 - Schaeffer pluton)																						
1	0.05446	0.00168	0.43702	0.01491	0.05833	0.00068	0.34	390	67.63	368.1	10.53	365.5	4.12	0	1	5719	312	1656	37428	706	105923	0.35
2	0.0543	0.00222	0.43421	0.01968	0.05842	0.00091	0.34	383.2	88.68	366.2	13.93	366	5.56	0	7	6499	354	1317	28730	805	120218	0.24
3	0.05287	0.00183	0.41777	0.01598	0.05851	0.00077	0.34	323.3	76.81	354.5	11.44	366.6	4.66	0	0	7890	418	1676	39329	989	145766	0.27
4	0.05301	0.002	0.41939	0.01728	0.05887	0.0008	0.33	329.2	83.27	355.6	12.36	368.8	4.88	0	10	2935	156	1046	25817	367	53912	0.48
5	0.05321	0.00157	0.41313	0.01338	0.05887	0.00064	0.34	337.6	65.73	351.1	9.61	368.8	3.9	7	45	3583	191	1107	27347	457	65825	0.42
6	0.05306	0.00266	0.41713	0.02276	0.05858	0.00103	0.32	331.2	109.7	354	16.31	367	6.29	21	4	1807	96	628	14835	228	33382	0.44
7	0.05283	0.00096	0.43232	0.00873	0.05905	0.00042	0.35	321.6	40.87	364.8	6.19	369.8	2.54	29	16	10381	549	2978	67724	1259	190273	0.36
8	0.05549	0.00085	0.45132	0.0077	0.05804	0.00036	0.36	431.6	33.31	378.2	5.39	363.7	2.2	9	0	16765	932	4251	95879	2046	312705	0.31
9	0.05384	0.00126	0.4231	0.01086	0.05862	0.00052	0.35	364.3	51.74	358.3	7.75	367.2	3.17	4	0	5979	322	1820	42502	755	110446	0.38
10	0.05573	0.00116	0.45509	0.01049	0.05857	0.00047	0.35	441.5	45.24	380.8	7.32	366.9	2.87	37	0	7095	396	2149	52349	863	131207	0.40
11	0.05589	0.00131	0.45395	0.01186	0.05839	0.00054	0.35	447.6	51.11	380	8.28	365.8	3.28	0	8	11508	643	4415	102378	1408	213577	0.48
12	0.05346	0.00085	0.42803	0.00753	0.05855	0.00037	0.36	348.1	35.48	361.8	5.36	366.8	2.26	89	0	16699	893	3863	90760	2073	309150	0.29
13	0.05424	0.0021	0.42517	0.01809	0.05749	0.00082	0.34	380.8	84.21	359.7	12.89	360.3	4.99	0	0	3544	192	1329	29775	449	66853	0.45
14	0.05569	0.0015	0.44192	0.0131	0.0583	0.00059	0.34	439.6	58.53	371.6	9.22	365.3	3.62	0	0	4631	258	1527	35947	580	86139	0.42
15	0.05351	0.003	0.43458	0.02706	0.05831	0.00124	0.34	350.2	121.5	366.4	19.15	365.3	7.55	0	0	4386	234	1356	33095	537	81601	0.41
16	0.05405	0.0011	0.45689	0.01036	0.06077	0.00049	0.36	373	45.06	382.1	7.22	380.3	2.96	0	23	16136	872	3675	84489	1900	288186	0.29
17	0.05337	0.00155	0.41229	0.01319	0.05835	0.00065	0.35	344.3	64.48	350.5	9.49	365.6	3.94	0	23	8747	466	3501	82236	1127	162738	0.51
18	0.05444	0.00141	0.43315	0.01242	0.05884	0.00059	0.35	389.3	56.9	365.4	8.8	368.5	3.57	0	0	6851	372	1804	38865	857	126440	0.31
19	0.05496	0.00187	0.43376	0.01631	0.05857	0.00076	0.35	410.5	73.68	365.8	11.55	366.9	4.64	81	19	6484	356	2199	45398	818	120240	0.38
20	0.05387	0.0015	0.44244	0.0137	0.05848	0.00063	0.35	365.6	61.42	372	9.65	366.3	3.83	51	0	13501	726	3560	81262	1638	250832	0.32
Sample 4 (88LHA-17-08 - Hoidahl Cupola)																						
1	0.05399	0.00059	0.43607	0.00529	0.05871	0.00027	0.38	370.5	24.58	367.5	3.74	367.8	1.66	20	13	33825	1852	5875	135937	4091	614282	0.22
2	0.05384	0.00062	0.43396	0.00557	0.0585	0.00028	0.37	364.4	25.99	366	3.95	366.5	1.73	0	12	25591	1397	2216	52171	3102	466512	0.11
3	0.05414	0.00101	0.43496	0.00905	0.05841	0.00043	0.35	376.6	41.6	366.7	6.41	365.9	2.64	1	31	16518	906	2941	69217	2009	301687	0.23
4	0.05269	0.00093	0.41188	0.00806	0.05828	0.00041	0.36	315.6	39.7	350.2	5.8	365.1	2.49	6	0	23688	1265	2002	46338	2962	433698	0.11
5	0.05689	0.00112	0.45825	0.01009	0.0587	0.00047	0.36	486.8	43.14	383	7.03	367.7	2.85	0	3	21110	1217	1619	42073	2563	383821	0.11
6	0.0542	0.00089	0.43074	0.00787	0.05875	0.00039	0.36	379.1	36.69	363.7	5.58	368	2.36	0	16	17246	946	2029	49305	2123	313443	0.16
7	0.05386	0.00118	0.42749	0.01036	0.05769	0.0005	0.36	365.2	48.52	361.4	7.37	361.6	3.02	58	5	18895	1030	1151	33618	2330	349806	0.10
8	0.0532	0.00078	0.41897	0.00677	0.05641	0.00033	0.36	337.1	32.67	355.3	4.85	353.8	2.03	13	21	24571	1323	2227	52600	3054	465418	0.11
9	0.05184	0.00081	0.42233	0.00728	0.0588	0.00036	0.36	278.5														

Sample 5 (88LHA-1-4B - Mt. Fitton pluton)																						
1	0.05447	0.00037	0.41739	0.00335	0.05627	0.00015	0.33	390.5	15.17	354.2	2.4	352.9	0.93	1	58	299542	15837	54934	766546	20758	2551692	0.30
2	0.05494	0.00037	0.41404	0.00333	0.05604	0.00015	0.33	409.8	15.28	351.8	2.39	351.5	0.93	12	92	253323	13515	60327	972895	17849	2169226	0.45
3	0.0549	0.0003	0.46281	0.00297	0.06187	0.00014	0.35	408	12	386.2	2.06	387	0.83	95	12	273295	14571	37483	506387	17213	2120758	0.24
4	0.05579	0.00029	0.36388	0.00214	0.04983	0.00011	0.38	443.6	11.56	315.1	1.59	313.5	0.65	6	5	259907	14092	28129	527571	21155	2509493	0.21
5	0.05363	0.00024	0.36329	0.00175	0.0496	0.00009	0.38	355.4	9.88	314.7	1.3	312.1	0.54	63	7	313424	16339	34259	587124	24563	3041690	0.19
6	0.05584	0.00031	0.43226	0.00284	0.05865	0.00013	0.34	445.5	12.43	364.8	2.01	367.4	0.81	14	25	171365	9304	34882	493864	11751	1408055	0.35
7	0.05339	0.0003	0.43636	0.00291	0.05902	0.00013	0.33	345.4	12.73	367.7	2.06	369.6	0.82	19	7	277561	14423	22979	325204	18025	2272478	0.14
8	0.05706	0.00039	0.41604	0.00336	0.05575	0.00015	0.33	493.3	15.17	353.2	2.41	349.7	0.94	106	26	153316	8520	40436	594333	11159	1331643	0.45
9	0.05216	0.00056	0.39103	0.00544	0.05406	0.00023	0.31	292.3	24.15	335.1	3.97	339.4	1.4	77	0	105357	5603	10776	137188	5405	637177	0.22
10	0.05345	0.00044	0.43315	0.00471	0.05861	0.0002	0.31	347.9	18.57	365.4	3.34	367.2	1.19	59	13	102262	5568	19510	221725	4859	570845	0.39
11	0.05334	0.00048	0.43007	0.00507	0.05896	0.00021	0.30	343.3	20.05	363.2	3.6	369.3	1.29	36	16	103122	5598	23021	249553	4930	572627	0.44
12	0.0527	0.00091	0.43537	0.01017	0.0586	0.00041	0.30	315.7	38.9	367	7.2	367.1	2.49	33	0	41686	2233	8804	102739	1947	233033	0.44
13	0.05236	0.00053	0.42253	0.00566	0.05866	0.00024	0.31	301	22.94	357.9	4.04	367.5	1.45	29	18	76617	4074	11131	121884	3668	428163	0.28
14	0.05334	0.00051	0.41789	0.00521	0.05612	0.00021	0.30	343.4	21.3	354.5	3.73	352	1.3	0	0	73517	3976	14796	177146	3634	429946	0.41
15	0.05358	0.00051	0.43476	0.00546	0.0589	0.00022	0.30	353.4	21.29	366.5	3.86	368.9	1.37	7	0	50501	2740	8620	123495	2413	281589	0.44
16	0.05186	0.00045	0.39718	0.00441	0.05503	0.00019	0.31	279.2	19.55	339.6	3.2	345.3	1.14	35	0	95794	5027	19428	238418	4854	572121	0.42
17	0.05182	0.00066	0.42085	0.00711	0.05893	0.0003	0.30	277.6	28.91	356.7	5.08	369.1	1.82	6	0	94135	4932	38523	432418	4504	525330	0.82
18	0.05284	0.0004	0.42682	0.00424	0.05873	0.00018	0.31	321.9	17.32	360.9	3.02	367.9	1.09	16	14	93931	5013	37284	403328	4523	526331	0.77
19	0.05427	0.00042	0.36816	0.00359	0.04935	0.00015	0.31	382.3	17.83	318.3	2.66	310.5	0.92	0	41	102208	5587	13015	181176	5881	682926	0.27
20	0.05318	0.00057	0.43224	0.00614	0.05853	0.00025	0.30	336.5	24.11	364.8	4.35	366.7	1.53	30	26	72313	3869	11909	142539	3477	407603	0.35
21	0.05401	0.00059	0.40071	0.00574	0.05503	0.00024	0.30	371.1	24.7	342.2	4.16	345.4	1.48	0	0	104455	5670	20717	276289	5508	626601	0.44
22	0.05255	0.00061	0.38811	0.00584	0.05349	0.00025	0.31	309.3	26.14	333	4.27	335.9	1.51	12	37	129496	6834	18048	208717	6868	799768	0.26
23	0.05285	0.0005	0.42108	0.00519	0.05868	0.00022	0.30	322.5	21.28	356.8	3.71	367.6	1.34	0	23	82357	4367	15395	170774	4054	463938	0.37
24	0.05282	0.00051	0.41171	0.0052	0.05498	0.00021	0.30	321.1	21.84	350.1	3.74	345	1.29	16	0	91094	4818	14494	174236	4594	548449	0.32
25	0.05327	0.00051	0.43536	0.00546	0.05867	0.00022	0.30	340.3	21.42	367	3.86	367.6	1.36	0	12	55517	2958	11664	128876	2673	313392	0.41
26	0.05277	0.00057	0.36912	0.00518	0.04968	0.00021	0.30	319	24.54	319	3.84	312.5	1.31	41	0	88707	4679	10795	136969	4997	591815	0.23
27	0.05379	0.00072	0.44234	0.00793	0.05844	0.00032	0.31	361.9	30.13	371.9	5.58	366.1	1.92	46	0	75206	4039	11891	138670	3607	426827	0.32
28	0.05451	0.00064	0.41645	0.00647	0.05508	0.00026	0.30	392.3	26.2	353.5	4.64	345.7	1.59	57	0	64292	3496	10589	133323	3324	387336	0.34

Sample 6 (C-194566 - Ammerman granite)																						
1	0.05552	0.00086	0.45791	0.00811	0.05917	0.00037	0.35	432.9	33.75	382.8	5.65	370.6	2.23	70	18	21944	1213	6467	147746	1942	491355	0.30
2	0.05426	0.00088	0.44271	0.0082	0.05911	0.00038	0.35	381.7	36.17	372.2	5.77											

15	0.05518	0.00093	0.44698	0.00869	0.05914	0.0004	0.35	419.4	36.86	375.2	6.1	370.4	2.45	0	15	21679	1196	7470	174020	2035	499608	0.35
16	0.05414	0.00085	0.43339	0.00793	0.05861	0.00038	0.35	376.7	35.23	365.6	5.62	367.1	2.31	22	0	30024	1625	11556	274938	2858	699197	0.39
Sample 7 (C-194567 - Ammerman quartz porphyry)																						
1	0.05316	0.00064	0.45096	0.00612	0.06112	0.00033	0.40	335.6	26.99	378	4.29	382.5	2.01	53	0	39651	2119	3715	127967	4270	971153	0.13
2	0.0537	0.00044	0.44336	0.0041	0.0592	0.00025	0.46	358.2	18.52	372.6	2.88	370.7	1.54	0	0	68954	3723	11074	347576	7632	1744906	0.20
3	0.05297	0.00081	0.43377	0.00748	0.05845	0.00038	0.38	327.5	34.37	365.9	5.3	366.2	2.31	1	13	26937	1435	15863	522112	3007	690813	0.76
4	0.05466	0.00123	0.45437	0.01154	0.05877	0.00052	0.35	398.5	49.3	380.3	8.06	368.1	3.18	40	0	5201	285	1294	41969	572	132730	0.32
5	0.05336	0.00068	0.44742	0.00643	0.05991	0.00034	0.39	344.2	28.54	375.5	4.51	375.1	2.05	30	0	18342	984	7897	276287	2001	459477	0.60
6	0.05153	0.00091	0.42089	0.00827	0.05889	0.00042	0.36	264.8	39.88	356.7	5.91	368.9	2.54	33	0	9577	496	3274	112695	1074	244389	0.46
7	0.05319	0.00076	0.44414	0.00716	0.05942	0.00036	0.38	337	32.04	373.2	5.04	372.1	2.22	41	21	14588	780	6789	228443	1600	369135	0.62
8	0.0541	0.00057	0.4487	0.00527	0.05921	0.00029	0.42	375.2	23.55	376.4	3.69	370.8	1.78	39	16	30763	1674	12966	439312	3400	781688	0.56
9	0.05393	0.00063	0.43671	0.0057	0.05932	0.00031	0.40	368	26.16	367.9	4.03	371.5	1.92	0	37	30344	1646	12204	420107	3436	770054	0.55
10	0.05334	0.00051	0.43869	0.0047	0.05944	0.00028	0.44	343	21.41	369.3	3.31	372.2	1.69	33	0	49339	2648	22821	755629	5503	1250358	0.60
11	0.05527	0.0009	0.44487	0.00816	0.05881	0.0004	0.37	422.9	35.54	373.7	5.73	368.4	2.45	22	0	10658	593	2953	101481	1215	273341	0.37
12	0.05401	0.00094	0.45019	0.0088	0.05933	0.00042	0.36	371.4	38.76	377.4	6.16	371.5	2.57	4	0	9336	507	2608	87700	1029	237513	0.37
13	0.05445	0.00086	0.46552	0.00827	0.06171	0.00041	0.37	389.5	34.75	388.1	5.73	386	2.48	30	7	12124	664	5241	178259	1303	296743	0.60
14	0.05446	0.00065	0.44391	0.00596	0.05865	0.00032	0.41	390.1	26.53	373	4.19	367.4	1.94	1	0	21028	1153	9884	320718	2371	541840	0.59
15	0.05232	0.00066	0.43224	0.00607	0.05989	0.00033	0.39	299.6	28.32	364.8	4.31	375	2.01	12	0	20292	1069	8262	275751	2259	512316	0.54
16	0.05322	0.00073	0.44152	0.00679	0.05985	0.00035	0.38	338.3	30.64	371.3	4.78	374.7	2.15	26	3	16396	878	5583	192388	1819	414751	0.46
17	0.05383	0.00116	0.44591	0.01086	0.05936	0.00052	0.36	363.8	48.09	374.4	7.62	371.7	3.14	0	2	12032	652	3511	119456	1337	307078	0.39
18	0.05355	0.00095	0.4392	0.0087	0.05914	0.00043	0.37	351.9	39.49	369.7	6.14	370.4	2.59	0	0	10723	578	2961	98724	1204	274873	0.36
19	0.05365	0.00155	0.43581	0.01407	0.05919	0.00065	0.34	356.3	63.83	367.3	9.95	370.7	3.97	0	2	4414	238	907	29850	500	113125	0.26
20	0.05206	0.00162	0.43701	0.01524	0.05963	0.0007	0.34	287.9	69.39	368.1	10.77	373.4	4.27	27	8	5086	266	1639	55228	558	129459	0.43
Sample 8 (88LHA-07-06 - Dave Lord pluton)																						
1	0.0546	0.00124	0.43054	0.01091	0.05833	0.00052	0.35	395.9	50.01	363.6	7.74	365.4	3.19	0	0	13809	768	3374	75442	1699	250792	0.30
2	0.05203	0.00126	0.42058	0.01125	0.05856	0.00054	0.34	286.6	54.2	356.5	8.04	366.9	3.29	0	9	12351	655	3563	83656	1483	223454	0.37
3	0.05388	0.00128	0.44336	0.01178	0.05845	0.00054	0.35	365.8	52.69	372.6	8.28	366.2	3.31	20	40	15269	838	4492	106426	1801	276868	0.38
4	0.05268	0.00087	0.43746	0.00804	0.05848	0.00038	0.35	315.1	37.03	368.5	5.68	366.4	2.31	0	23	12919	693	4372	104706	1510	234177	0.45
5	0.05367	0.00162	0.44143	0.01492	0.05811	0.00068	0.35	357	66.8	371.3	10.51	364.1	4.14	29	6	10067	550	3826	92731	1188	183683	0.50
6	0.05606	0.0016	0.43973	0.01397	0.05844	0.00066	0.36	454.4	62.24	370.1	9.85	366.1	3.99	26	0	7248	413	2113	52922	897	131569	0.40
7	0.05246	0.00104	0.4211	0.00919	0.05891	0.00045	0.35	305.6	44.27	356.8	6.56	369	2.72	14	0	7724	412	2298	53854	935	139136	0.39
8	0.052	0.00104	0.42462	0.0094	0.05869	0.00045	0.35	285.2	45.08	359.4	6.7	367.7	2.72	0	9	8200	434	2241	51620	976	148273	0.35
9	0.05389</																					

Sample 9 (91ADo-284 - Bear Mountain pluton)																						
1	0.04742	0.00152	0.05345	0.00167	0.00798	0.00008	0.32	69.9	75.39	52.9	1.61	51.2	0.54	0	32	3887	184	1148	287050	3114	717284	0.40
2	0.04639	0.00181	0.05296	0.00201	0.00804	0.0001	0.33	17.7	91.3	52.4	1.93	51.6	0.67	74	3	3452	160	838	200044	2732	632488	0.32
3	0.04598	0.00178	0.05197	0.00195	0.00789	0.0001	0.34	0.1	86.36	51.4	1.88	50.6	0.66	0	12	3575	164	1048	261581	2859	668231	0.39
4	0.04707	0.00196	0.05293	0.00214	0.00803	0.00011	0.34	52.4	96.95	52.4	2.06	51.5	0.72	45	0	2846	134	934	202615	2289	523018	0.39
5	0.04687	0.0014	0.0527	0.00153	0.00815	0.00009	0.38	42.3	70.22	52.2	1.47	52.3	0.54	36	10	5425	255	1209	285648	4364	982035	0.29
6	0.04478	0.00181	0.05259	0.00205	0.00827	0.00011	0.34	0.1	27.83	52	1.98	53.1	0.73	63	0	5632	253	1371	321168	4342	1006780	0.32
7	0.04708	0.00166	0.05367	0.00184	0.00817	0.0001	0.36	53	82.61	53.1	1.77	52.5	0.63	37	11	3770	178	980	222649	2995	682012	0.33
8	0.04328	0.00159	0.05053	0.00181	0.00822	0.0001	0.34	0.1	0	50	1.75	52.8	0.62	0	25	3661	159	906	206445	2842	659024	0.31
9	0.0472	0.00233	0.05424	0.0026	0.00819	0.00013	0.33	58.8	114.1	53.6	2.51	52.6	0.81	15	6	1991	94	563	135741	1571	360042	0.38
10	0.04749	0.00155	0.05485	0.00174	0.00827	0.00009	0.34	73.1	76.45	54.2	1.67	53.1	0.59	0	0	3075	146	806	193692	2415	550775	0.35
11	0.04817	0.00208	0.05574	0.00232	0.00833	0.00013	0.37	107.7	98.95	55.1	2.24	53.5	0.81	3	12	2638	127	717	187358	2069	469802	0.40
12	0.04761	0.00161	0.05602	0.00183	0.00838	0.0001	0.37	79.3	79.34	55.3	1.76	53.8	0.65	0	0	4951	236	1230	282548	3821	876855	0.32
13	0.04468	0.00226	0.05066	0.00249	0.00823	0.00013	0.32	0.1	45.91	50.2	2.4	52.8	0.86	0	1	2737	122	801	185508	2193	493897	0.38
14	0.04747	0.0014	0.05173	0.00147	0.00785	0.00008	0.36	72.4	69.44	51.2	1.42	50.4	0.54	0	8	7474	356	1638	369768	6234	1415828	0.26
15	0.04635	0.002	0.05301	0.00222	0.00812	0.00012	0.35	16	100.6	52.4	2.14	52.1	0.75	37	23	3033	141	800	193370	2411	555796	0.35
16	0.04636	0.00141	0.05289	0.00155	0.00811	0.00009	0.38	16.2	70.41	52.3	1.5	52.1	0.56	14	0	5275	245	1268	294792	4207	968655	0.30
17	0.04849	0.00124	0.05504	0.00137	0.00811	0.00008	0.40	123.1	59.3	54.4	1.31	52.1	0.49	0	1	4749	231	1351	312475	3809	872591	0.36
18	0.04667	0.00191	0.05335	0.00212	0.00812	0.00011	0.34	32.3	95.26	52.8	2.04	52.2	0.7	58	0	2949	138	905	215243	2350	541115	0.40
19	0.04851	0.0019	0.05568	0.00212	0.00818	0.00011	0.35	124.4	89.75	55	2.04	52.5	0.69	27	0	2452	119	650	153764	1947	447358	0.34
20	0.04793	0.00169	0.05468	0.00187	0.00812	0.0001	0.36	94.8	82.39	54.1	1.8	52.1	0.62	5	8	3214	154	1144	288594	2568	590863	0.49
Sample 10 (91ADo-279 - Bear Mountain rhyolite porphyry dyke)																						
1	0.04635	0.00111	0.05512	0.00128	0.00845	0.00007	0.36	15.9	55.78	54.5	1.23	54.3	0.46	0	8	8347	387	2559	527572	6268	1430338	0.37
2	0.04615	0.00082	0.05506	0.00095	0.00842	0.00006	0.41	5.3	42.19	54.4	0.92	54	0.37	62	0	15884	733	3370	731148	11892	2734658	0.27
3	0.04715	0.00076	0.05563	0.00086	0.00849	0.00005	0.38	56.6	37.11	55	0.83	54.5	0.34	0	0	12006	566	1595	352557	9095	2049550	0.17
4	0.04817	0.00124	0.05573	0.00139	0.00828	0.00008	0.39	107.6	59.73	55.1	1.33	53.2	0.5	13	36	8692	419	2878	641916	6716	1522729	0.42
5	0.04804	0.00093	0.05558	0.00104	0.0083	0.00006	0.39	101	44.97	54.9	1	53.3	0.39	0	10	16758	805	3282	774789	12954	2933051	0.26
6	0.04814	0.00124	0.05709	0.00142	0.00834	0.00008	0.39	106.3	59.54	56.4	1.36	53.5	0.5	44	0	6968	335	2001	431534	5260	1214865	0.36
7	0.04814	0.00101	0.05647	0.00115	0.0083	0.00007	0.41	106.4	48.86	55.8	1.1	53.3	0.42	41	0	10143	488	2440	523559	7745	1777196	0.29
8	0.0471	0.00124	0.05622	0.00143	0.0083	0.00008	0.38	53.9	61.91	55.5	1.38	53.3	0.49	30	0	4997	235	824	182226	3751	876139	0.21
9	0.04774	0.00087	0.05553	0.00098	0.0083	0.00006	0.41	85.3	43.8	54.9	0.95	53.3	0.37	8	0	16906	808	7518	1696745	13026	2966737	0.57
10	0.04703	0.00077	0.05496	0.00087	0.00832	0.00005	0.38	50.6	37.84	54.3	0.84	53.4	0.33	0	0	11931	561	2159	490774	9155	2090169	0.23
11	0.04696	0.00181	0.05564	0.00208	0.00833	0.00011	0.35	47.1	90.02	55	2	53.5	0.69	0	21	3761	176	1012	215737	2849	658698	0.33
12	0.04836	0.00242	0.05662	0.00274	0.00846	0.00015	0.37	116.9	114.1	55.9	2.64	54.3	0.95	0	24	4589	222</					